ILLUMINATING SUPEROXIDE PATHWAYS IN IRRADIATED NATURAL WATERS USING VARIED CHEMICAL PARAMETERS

by

KANDIS MARIE ARLINGHAUS

(Under the Direction of William L. Miller)

ABSTRACT

Superoxide (O_2^-) is a reactive oxygen species (ROS) that is primarily produced by the one-electron transfer of photo-oxidized colored dissolved organic matter (CDOM) in sunlit natural waters. Superoxide has dual oxidative and reducing properties to control the fate of oxygen and subsequent photochemically-mediated redox reactions. Here we examine the environmental and chemical parameters that control O_2^- photochemical decay pathways in natural water using the enzyme superoxide dismutase (SOD). Freshwater samples were used to establish a reproducible natural photochemical source material and then augmented chemically to mimic specific seawater constituents (ionic strength, buffer, halides, and pH). SOD was used to compare redox pathways and infer maximal O_2^- photoproduction rates from H_2O_2 measurements quantified by flow injection chemiluminescent analysis. These results will help illuminate the parameters that control O_2^- pathways in irradiated samples and deepen our understanding of the role of photochemistry in biogeochemical cycles and the redox state of sunlit waters.

INDEX WORDS: Photochemistry, Reactive oxygen species (ROS), Superoxide, Flow injection analysis, Chemiluminescence

ILLUMINATING SUPEROXIDE PATHWAYS IN IRRADIATED NATURAL WATERS USING VARIED CHEMICAL PARAMETERS

by

KANDIS MARIE ARLINGHAUS

B.S., BELLARMINE UNIVERSITY, 2019

A Thesis Submitted to the Graduate Faculty of The University of Georgia in Partial Fulfillment of the Requirements for the Degree

MASTER OF SCIENCE

ATHENS, GEORGIA

2022

ILLUMINATING SUPEROXIDE PATHWAYS IN IRRADIATED NATURAL WATERS USING VARIED CHEMICAL PARAMETERS

by

KANDIS MARIE ARLINGHAUS

Major Professor:	William L. Miller
Committee:	Amanda Frossard Leanne Powers

Electronic Version Approved:

Ron Walcott
Vice Provost for Graduate Education and Dean of the Graduate School
The University of Georgia
May 2022

DEDICATION

I would like to dedicate this work to my parents for encouraging my passion for the water ever since I was young and to my sister for being my biggest champion and scientist role model.

ACKNOWLEDGEMENTS

I would first like to thank my advisor, Bill Miller, for his enthusiastic support and passionate spirit. Thank you for going above and beyond to foster an environment for learning and always divulging in enlightening conversations. Second, I would like to thank my co-advisor and committee member, Amanda Frossard, for her generous encouragement and invaluable guidance throughout my time at UGA. I am eternally grateful to have been welcomed into your lab group and be presented with the opportunity to join the Bermuda research cruise. Third, I would like to thank my committee member and Miller lab predecessor, Leanne Powers, for her kindness, insightful suggestions, and overflowing wisdom of our infamous instrument, the "mini-Lume".

Next, I would like to thank the faculty and staff of UGA Marines Sciences. Thank you for your leadership and direction throughout my courses and research. I especially want to thank Adrian Burd for his perceptive and generous mentorship. Also, thank you Marc Frischer, Adam Greer, and the crew of the R/V Savannah for my first research cruise opportunity; I loved every moment of living and "sciencing" at sea. Additionally, I would like to thank my fellow grad students, both in Marine Sciences and in the Frossard Lab. Thank you for always being a source of solace and inspiration during the ebbs and flows of graduate school.

Lastly, I would like to thank my friends and family who continually endorse my passion for the ocean and all things water, especially my parents, sister, and Bellarmine Swim family.

TABLE OF CONTENTS

Page

LIST OF TABLES

Page

LIST OF FIGURES

Page

CHAPTER 1

INTRODUCTION AND LITERATURE REVIEW

1. Aquatic Photochemistry

Solar radiation drives unique chemical reactions in the environment, ultimately creating diel cycles of photochemical intermediates and transient species. Natural surface waters are subject to these reactions more so than underlying waters due to attenuation and scattering that decreases photon absorption with depth in the water column (Zafiriou et al., 1984). One of the major light-absorbing substances responsible for photochemical processes in the surface waters is colored or chromophoric dissolved organic matter (CDOM; Plane et al., 1997; Clark & Zika, 2000). Operationally, CDOM represents the light absorbing fraction of dissolved constituents in natural waters and is measured in units of 1/meter (m^{-1}). The majority of this absorbance is thought to be primarily composed of aromatic amino acids, lignin phenols, and undefined humic substances (Sharpless & Blough, 2014; Zhang et al., 2021). CDOM contributes to the optical properties of natural waters, alters nutrient availability, and consequently is significant in processes that affect the global carbon cycle. Although knowledge of CDOM optical abundance, chemical characteristics, and environmental effects has rapidly grown in the past 30 years, its full impact on aquatic systems remains poorly understood due to its complex structures and interdisciplinary ecological implications (Clark & Zika, 2000; Coble, 2008; Zhang et al., 2021).

Optical, isotope, and mass spectrometric techniques can be used to describe CDOM abundance, composition, and sources. However, the variable sources and chemical structures of CDOM compounds make it difficult to know which specific phenolic moieties and surface-active

properties to isolate for characterization (Plane et al., 1997; Zhang et al., 2021). For this reason, CDOM has yet to be fully chemically defined, and the molecular composition and percentage of CDOM in the DOM pool are difficult to establish (Coble, 2008). Additionally, light absorption and CDOM quantities are described by optical units, using the absorption coefficient ($a(\lambda)$; m^{-1}) spectrum, instead of molar concentrations (mol/L), making it difficult to contextualize in environmental systems (Clark & Zika, 2000). CDOM absorption coefficients must be determined at different wavelengths or wavebands suitable to the individual aims of different studies, thus making interstudy comparisons difficult (Twardowski et al., 2004; Zhang et al., 2021).

The spectra of CDOM light absorption typically decreases exponentially with increasing wavelength and can be defined using the following equations:

$$a(\lambda) = a(\lambda o)e^{-S(\lambda-\lambda o)} \quad (1)$$

$$a(\lambda) = 2.303\ A(\lambda)/r \quad (2)$$

where $a(\lambda)$ and $a(\lambda o)$ are the absorption coefficients at wavelengths λ and a reference wavelength λo; S is the spectral slope parameter; and A is the absorbance in a spectrophotometer with path length, r, in meters (Blough et al., 1997; Clark & Zika, 2000; Twardowski et al., 2004). Aspects of this exponential absorbance spectrum, and potential indications of inherent chemical characteristics, can be represented using absorption ratios at reference wavelengths. Commonly used ratios for CDOM absorption include E2/E3 (Abs_{254}/Abs_{365}) and E4/E6 (Abs_{465}/Abs_{665}), which can serve as proxies to characterize aquatic humic substances (Peuravuori & Pihlaja, 1997; Dalrymple et al., 2010; Sharpless & Blough, 2014).

The bioavailability and distribution of CDOM in natural waters is largely driven by the cycling of its sources and sinks. CDOM composition, and thus its photoreactivity, is highly dependent on its source material. Soils from rivers and groundwaters are a primary source for

CDOM in both freshwater (Zhang et al., 2021) and coastal seawater (Coble, 2008). Microbial decomposition, sediment release, atmospheric deposition, and anthropogenic inputs are also potential sources in these, and oceanic waters. The variability in sources between inland, coastal, and open ocean aquatic systems can give rise to photoreactivity differences. On the other side of the balance, CDOM loss is dominated by photobleaching, which results in a decrease in the absorption coefficient of CDOM across all wavelengths and permits increased light penetration and euphotic zone depths in the water column (Coble, 2008; Zhang et al., 2021).

Variability in source material is just one of many environmental factors that can influence aquatic photochemistry. Seasonal dynamics in meteorological and hydrological processes, such as photobleaching, precipitation, and inflow runoff, can affect CDOM abundance and composition and ultimately result in varied photochemical reactivity (Zhang et al., 2021). Changes in pH or ionic strength can alter organic structural conformation due to changing charge distributions and subsequently affect optical properties and the potential for electron transfer. Specifically, DOM polymers and colloids condense at low pH and high salinities, limiting light exposure. In contrast, DOM expands at higher pH and lower salinities, resulting in greater initial light absorption (Spencer et al., 2007; Pace et al., 2012; Lu et al., 2015).

CDOM is highly photoreactive, acting as both a substrate and sensitizer for direct (primary) and indirect (secondary) phototransformations (Plane et al., 1997; Blough, 1997). The photophysics and photochemistry of CDOM are complex; stemming directly from the complex mixture of absorbing compounds that define CDOM. Various reactions can result in “excited” molecular states, charge-separated species, and radical forms. Homolytic bond cleavage, formation of diradical charge-separated species, and oxidation by O_2 are thought to be the main mechanisms responsible for CDOM radical production during irradiation (Sharpless & Blough,

2014). These charged molecules can then participate in further electron transfer with nearby oxygen molecules to produce various reactive oxygen species (ROS) such as singlet oxygen ($^1O_2$), superoxide (O_2^-), hydrogen peroxide (H_2O_2), and hydroxyl radical (•OH; Sharpless & Blough, 2014). These photochemical reactions can propel an array of relevant environmental reactions such as the biogeochemical cycling of carbon, redox-sensitive trace elements, and gases, potentially altering the bulk redox potential of surface waters with subsequent influence on biological activity and global climate (Coble, 2008; Zhang et al., 2021).

2. Reactive Oxygen Species (ROS)

The first study to report ROS, specifically H_2O_2, in surface seawater was in 1966 (Van Baalen & Marler, 1966). In the 1980s, a multitude of evidence supported the notion that the main source of ROS in natural water is by abiotic photochemical excitation of CDOM and its subsequent reactions with oxygen (Zepp & Schlotzhauer, 1981; Blough & Zepp, 1995). While scientific advancements have since strengthened our understanding of the sources and sinks of ROS, many aspects of specific ROS reactions remain to be explored that would improve kinetic models of the complex role of ROS in environmental redox processes and help predict climate relevant impacts.

ROS are free radical molecules produced by redox reactions or electron excited states in oxygen. These molecules are highly reactive because they contain at least one unpaired electron in their outer valence shell, potentially changing their total spin and giving them a higher affinity to donate or accept another electron to achieve stability (Ho et al., 1995). They exist as extracellular and intracellular transient species produced by both chemical and biological processes. In irradiated surface waters, they are primarily produced by the photoexcitation of

CDOM though they can also be produced by abiotic oxidation of reduced metals (Bielski et al., 1985; Kieber et al., 2003) and organismal respiration, photosynthesis, and enzymatic catalysis (Lesser, 2006; Hansel & Diaz, 2021).

ROS participate in critical redox reactions in both freshwater and seawater ecosystems. The most notable of these is their contribution to nutrient (carbon, oxygen, sulfur, nitrogen) and trace metal cycling (Blough & Zepp, 1995). The availability of these biologically important redox-active compounds is highly dependent on the redox state of the aquatic environments in which they occur (Kieber et al., 2003; Zepp et al., 2007). Additionally, ROS are known to cause direct oxidative damage to cells, proteins, and DNA in aquatic organisms (Lesser, 2006; Zepp et al., 2007; Hansel & Diaz, 2021); as well as altering the toxicity of, and creating new, organic pollutants (Scully et al., 2003; Richard & Canonica, 2005).

3. Superoxide (O_2^-)

Superoxide represents the initial one-electron reduction of O_2 and is the precursor for subsequent ROS production in natural waters. It is primarily produced during CDOM photo-oxidation caused by ultraviolet radiation (280–400 nm) absorption (Eq. 3; Burns et al., 2012). Marine photochemistry, however, is not the only source of O_2^- in the ocean. Superoxide can also be produced by the redox cycling of transition metals (Eq. 4; Burns et al., 2012), enzymatic reactions (e.g. xanthine oxidase; Bielski et al., 1985), and biological respiration of microorganisms (Sutherland et al., 2020; Hansel & Diaz, 2021).

$$CDOM + O_2 + h\nu \rightarrow CDOM^+_{oxid} + O_2^- \quad (3)$$

$$M^{n+} + O_2 \rightarrow M^{(n+1)+} + O_2^- \quad (4)$$

Superoxide pathways can control the fate of molecular O_2 by its ability to act as either a one-electron reductant or oxidant. If O_2^- donates an electron via an oxidative pathway, then the oxygen molecule returns to the dissolved O_2 pool (Eq. 5). If O_2^- accepts an electron via a reductive pathway, then the oxygen molecule becomes H_2O_2 (Eq. 6; Ho et al., 1995; Goldstone & Voelker, 2000). An uncatalyzed dismutation reaction also exists for O_2^- and its conjugate acid, HO_2, in which O_2^- is reduced to form molecular O_2, H_2O_2, and OH^- (Eq. 7; Bielski et al., 1985).

Oxidation: $$O_2^- + Y_{ox} \rightarrow O_2 + Y_{red} \quad (5)$$

Reduction: $$O_2^- + X_{red} + 2H^+ \rightarrow H_2O_2 + X_{ox} \quad (6)$$

Dismutation: $$O_2^- + HO_2 + H_2O \rightarrow H_2O_2 + O_2 + OH^- \quad (7)$$

Subsequent reductive pathways of H_2O_2 can then result in hydroxyl radical (•OH) and eventually H_2O. Furthermore, extracellular O_2^- production has been identified as being responsible for 5–19% of O_2 sinks in the marine oxygen budget (Sutherland et al., 2020). Should superoxide reduction pathways dominate, major O_2 loss in the marine oxygen cycle would occur. This potential to direct future photochemically-mediated redox reactions is why O_2^- is considered a "gatekeeper" for subsequent redox reactions, and thus, a key intermediate in the cycling of organic matter and trace metals in sunlit waters (Powers & Miller, 2016).

Superoxide steady-state concentrations and production/decay rates in natural waters have been investigated over the past few decades. Steady-state concentration for O_2^- has been defined as the balance of production and decay rates as follows:

$$[O_2^-]_{ss} = \frac{\text{production}}{2k_D[O_2^-]_{ss} + \sum k_M[M]_x + k_{pseudo}} \quad (8)$$

where k_D (M^{-1} s^{-1}) is the pH dependent dismutation rate constant, k_M is the second-order rate constant with metal species M_x, and k_{pseudo} (s^{-1}) is the sum of pseudo-first-order rate constants with additional unknown sinks (Goldstone & Voelker et al., 2000).

Many researchers have measured and calculated $[O_2^-]_{ss}$ and decay rates in seawater to better understand O_2^- reactions. Reported superoxide steady-state concentrations range from 0.01–86 nM and decay rates vary from 0.0001–0.2 s^{-1}, though many of the O_2^- decay studies were experimentally catalyzed by trace metals (e.g. Cu, Fe, and Mn) or organic matter (outlined in Fuji and Otani, 2017). Results from these studies suggested interactions with metal compounds (Voelker et al., 2000; Heller & Croot, 2010b; Wuttig et al., 2013) and organic species with aromatic moieties (i.e. antioxidants, CDOM) such as quinones, phenols/polyphenols, or humics (Voelker et al., 2000; Heller & Croot, 2010a; Heller et al., 2016; Fujji & Otani, 2017; Ma et al., 2020) as potential abiotic sinks for O_2^- in seawater. The concentration and characteristics of these potential antioxidants for O_2^- in natural waters, however, are poorly understood. A study by King et al. (2016) presented an analytical method to estimate O_2^- "antioxidant" activity in naturals waters. While this method does not identify the antioxidant species in their samples, and in fact measures any process that removes O_2^- from solution, the authors allude to photochemically activated organic species as a potential source for effective "antioxidant" activity. Working in the South Atlantic, they observed 0.1–0.4 nM of "antioxidants" in surface seawater samples collected during the day with a half-life of 3–7 min in the dark, consistent with photo-reactive species capable of scavenging superoxide.

Superoxide decay has been further explored using the enzyme superoxide dismutase (SOD) to determine the relationship between oxidative and reductive pathways (Petasne & Zika, 1987; Shaked et al., 2010; Garg et al., 2011; Powers & Miller, 2014; Powers & Miller, 2016).

Estimates of O_2^- production and decay rates were determined using 2:1 stoichiometry from measured H_2O_2 (Eq. 9; Burns et al., 2012).

$$2O_2^- + 2H^+ \text{—SOD}\rightarrow O_2 + H_2O_2 \quad (9)$$

Several of these studies suggest that dismutation to H_2O_2 (reductive pathway) may not always be the primary sink for O_2^-, as once assumed, and that oxidative pathways make up between 40–70% of O_2^- reactions in seawater (Petasne & Zika, 1987; Garg et al., 2011; Powers & Miller, 2016). Therefore, this 2:1 assumption applied to H_2O_2 measurements in-situ could grossly underestimate the predicted photochemical rates of superoxide. However, this oxidative sink predominance has not been observed across all systems. Photochemical experiments in the Gulf of Aqaba (Shaked et al., 2010) and a limited study from the Gulf of Alaska (Powers & Miller, 2014) found no effect of SOD on H_2O_2 photoproduction, thus suggesting O_2^- reduction to H_2O_2 as the dominant decay pathway.

These observations of predominant oxidative decay pathways for O_2^- are further supported by work using a single electron probe in irradiated solutions. Recent evidence has been presented showing one electron-reductants (OER) are formed during the initial photoexcitation and intramolecular electron transfer of CDOM that react with dissolved O_2 to form O_2^- (Zhang et al., 2012). Two studies from the same group used a nitroxide radical probe (3AP) to determine OER photoproduction rates, and thereby estimate O_2^- formation across standard humic and fulvic materials, as well as natural organic matter in freshwater (Zhang & Blough, 2016; Le Roux et al., 2021). Both studies suggested a significant oxidative sink for O_2^- around 65–88% that they suggest is caused by the simultaneous photoproduction of phenoxy radicals with CDOM. Thus, there is an apparent need for additional studies to illuminate relevant mechanisms and ROS kinetics stemming from the photo-oxidation of CDOM.

4. Thesis Overview

In this study, we aim to determine the environmental and chemical parameters that control superoxide photochemical pathways by comparing SOD stoichiometry to natural samples without the enzyme. This work will fill gaps in ROS kinetic data by exploring O_2^- pathways in irradiated freshwater and seawater samples using flow injection chemiluminescent analysis. Freshwater lake samples were used to establish a reproducible natural photochemical source material and then augmented chemically to mimic specific seawater constituents (ionic strength, buffer, halides, and pH). SOD is used to compare redox pathways and infer maximal O_2^- photoproduction rates from H_2O_2 measurements with varied experimental solutions. These results will help illuminate the environmental and chemical parameters that control O_2^- reaction pathways in irradiated samples and identify additional studies that are needed to model ROS kinetics. Furthermore, this study will deepen our understanding of the role of photochemistry in biogeochemical cycles and the redox state of sunlit waters.

Objectives:

1. Determine the environmental and chemical parameters that control superoxide decay pathways and maximal production rates
2. Understand how these decay pathways and rates change as the sample is continually irradiated

References

Bielski, B. H., Cabelli, D. E., Arudi, R. L., & Ross, A. B. (1985). Reactivity of HO2/O− 2 radicals in aqueous solution. *Journal of physical and chemical reference data, 14*(4), 1041-1100. doi: 10.1063/1.555739

Blough, N. (1997). Photochemistry in the sea-surface microlayer. In P. S. Liss & R. A. Duce (Eds.), *The Sea Surface and Global Change* (pp. 383-424): Cambridge University Press.

Blough, N. V., & Zepp, R. G. (1995). Reactive oxygen species in natural waters. In *Active oxygen in chemistry* (pp. 280-333): Springer. doi:10.1007/978-94-007-0874-7_8

Burns, J. M., Cooper, W. J., Ferry, J. L., King, D. W., DiMento, B. P., McNeill, K., Miller, C. J., Miller, W. L., Peake, B. M., Rusak, S. A., Rose, A. L., & Waite, T. D. (2012). Methods for reactive oxygen species (ROS) detection in aqueous environments. *Aquatic Sciences, 74*(4), 683-734. doi: 10.1007/s00027-012-0251-x

Clark, C. D., & Zika, R. G. (2000). Marine organic photochemistry: from the sea surface to marine aerosols. In *Marine Chemistry* (pp. 1-33): Springer. doi:10.1007/10683826_1

Coble, P. G. (2008). Marine Optical Biogeochemistry: The Chemistry of Ocean Color. *Chemical reviews, 107*(2), 402-418. doi: 10.1021/cr050350

Dalrymple, R. M., Carfagno, A. K., & Sharpless, C. M. (2010). Correlations between Dissolved Organic Matter Optical Properties and Quantum Yields of Singlet Oxygen and Hydrogen Peroxide. *Environmental science & technology, 44*(15), 5824-5829. doi: 10.1021/es101005u

Fujii, M., & Otani, E. (2017). Photochemical generation and decay kinetics of superoxide and hydrogen peroxide in the presence of standard humic and fulvic acids. *Water Research, 123*, 642-654. doi: 10.1016/j.watres.2017.07.015

Garg, S., Rose, A. L., & Waite, T. D. (2011). Photochemical production of superoxide and hydrogen peroxide from natural organic matter. *Geochimica et Cosmochimica Acta, 75*(15), 4310-4320. doi: 10.1016/j.gca.2011.05.014

Goldstone, J. V., & Voelker, B. M. (2000). Chemistry of superoxide radical in seawater: CDOM associated sink of superoxide in coastal waters. *Environmental science & technology, 34*(6), 1043-1048. doi: 10.1021/es9905445

Hansel, C. M., & Diaz, J. M. (2021). Production of extracellular reactive oxygen species by marine biota. *Annual review of marine science, 13*, 177-200. doi: 10.1146/annurev-marine-041320-102550

Heller, M., & Croot, P. (2010a). Kinetics of superoxide reactions with dissolved organic matter in tropical Atlantic surface waters near Cape Verde (TENATSO). *Journal of Geophysical Research: Oceans, 115*(C12). doi: 10.1029/2009JC006021

Heller, M. I., & Croot, P. L. (2010b). Superoxide decay kinetics in the Southern Ocean. *Environmental science & technology, 44*(1), 191-196. doi: 10.1021/es901766r

Heller, M. I., Wuttig, K., & Croot, P. L. (2016). Identifying the sources and sinks of CDOM/FDOM across the Mauritanian Shelf and their potential role in the decomposition of superoxide (O2-). *Frontiers in Marine Science, 3*, 132. doi: 10.3389/fmars.2016.00132

Ho, R. Y., Liebman, J. F., & Valentine, J. S. (1995). Overview of the Energetics and Reactivity of Oxygen. In *Active Oxygen in Chemistry* (pp. 1-23): Springer. doi:10.1007/978-94-007-0874-7_1

Kieber, D. J., Peake, B. M., & Scully, N. M. (2003). Reactive oxygen species in aquatic ecosystems. In E. W. Helbling & H. Zagarese (Eds.), *UV Effects in Aquatic Organisms and Ecosystems* (Vol. 1, pp. 251-288): The Royal Society of Chemistry. doi:10.1039/9781847552266-00251

King, D. W., Berger, E., Helm, Z., Irish, E., & Mopper, K. (2016). Measurement of antioxidant activity toward superoxide in natural waters. *Frontiers in Marine Science, 3*, 217. doi: 10.3389/fmars.2016.00217

Le Roux, D. M., Powers, L. C., & Blough, N. V. (2021). Photoproduction rates of one-electron reductants by chromophoric dissolved organic matter via fluorescence spectroscopy: comparison with superoxide and hydrogen peroxide rates. *Environmental science & technology, 55*(17), 12095-12105. doi: 10.1021/acs.est.1c04043

Lesser, M. P. (2006). OXIDATIVE STRESS IN MARINE ENVIRONMENTS: Biochemistry and Physiological Ecology. *Annual Review of Physiology, 68*(1), 253-278. doi: 10.1146/annurev.physiol.68.040104.110001

Lu, Q., Yuan, Y., Tao, Y., & Tang, J. (2015). Environmental pH and ionic strength influence the electron-transfer capacity of dissolved organic matter. *Journal of Soils and Sediments, 15*(11), 2257-2264. doi: 10.1007/s11368-015-1154-y

Ma, J., Nie, J., Zhou, H., Wang, H., Lian, L., Yan, S., & Song, W. (2020). Kinetic Consideration of Photochemical Formation and Decay of Superoxide Radical in Dissolved Organic Matter Solutions. *Environmental science & technology, 54*(6), 3199-3208. doi: 10.1021/acs.est.9b06018

Pace, M. L., Reche, I., Cole, J. J., Fernández-Barbero, A., Mazuecos, I. P., & Prairie, Y. T. (2012). pH change induces shifts in the size and light absorption of dissolved organic matter. *Biogeochemistry, 108*(1), 109-118. doi: 10.1007/s10533-011-9576-0

Petasne, R. G., & Zika, R. G. (1987). Fate of superoxide in coastal sea water. *Nature, 325*(6104), 516-518. doi: 10.1038/325516a0

Peuravuori, J., & Pihlaja, K. (1997). Molecular size distribution and spectroscopic properties of aquatic humic substances. *Analytica Chimica Acta, 337*(2), 133-149. doi: 10.1016/S0003-2670(96)00412-6

Plane, J., Blough, N., Ehrhardt, M., Water, K., Zepp, R., & Zika, R. (1997). Report Group 3 - Photochemistry in the sea-surface microlayer. In P. S. Liss & R. A. Duce (Eds.), *The Sea Surface and Global Change* (pp. 71-92): Cambridge Univ. Press.

Powers, L. C., & Miller, W. L. (2014). Blending remote sensing data products to estimate photochemical production of hydrogen peroxide and superoxide in the surface ocean. *Environmental Science: Processes & Impacts, 16*(4), 792-806. doi: 10.1039/C3EM00617D

Powers, L. C., & Miller, W. L. (2016). Apparent quantum efficiency spectra for superoxide photoproduction and its formation of hydrogen peroxide in natural waters. *Frontiers in Marine Science, 3*, 235. doi: 10.3389/fmars.2016.00235

Richard, C., & Canonica, S. (2005). Aquatic phototransformation of organic contaminants induced by coloured dissolved natural organic matter. In *Environmental Photochemistry Part II* (pp. 299-323): Springer. doi:10.1007/b138187

Scully, N. M., Cooper, W. J., & Tranvik, L. J. (2003). Photochemical effects on microbial activity in natural waters: the interaction of reactive oxygen species and dissolved organic matter. *FEMS microbiology ecology, 46*(3), 353-357. doi: 10.1016/S0168-6496(03)00198-3

Shaked, Y., Harris, R., & Klein-Kedem, N. (2010). Hydrogen peroxide photocycling in the Gulf of Aqaba, Red Sea. *Environmental science & technology, 44*(9), 3238-3244. doi: 10.1021/es902343y

Sharpless, C. M., & Blough, N. V. (2014). The importance of charge-transfer interactions in determining chromophoric dissolved organic matter (CDOM) optical and photochemical properties. *Environmental Science: Processes & Impacts, 16*(4), 654-671. doi: 10.1039/C3EM00573A

Spencer, R. G., Bolton, L., & Baker, A. (2007). Freeze/thaw and pH effects on freshwater dissolved organic matter fluorescence and absorbance properties from a number of UK locations. *Water Research, 41*(13), 2941-2950. doi: 10.1016/j.watres.2007.04.012.

Sutherland, K. M., Wankel, S. D., & Hansel, C. M. (2020). Dark biological superoxide production as a significant flux and sink of marine dissolved oxygen. *Proceedings of the National Academy of Sciences, 117*(7), 3433-3439. doi: 10.1073/pnas.1912313117

Twardowski, M. S., Boss, E., Sullivan, J. M., & Donaghay, P. L. (2004). Modeling the spectral shape of absorption by chromophoric dissolved organic matter. *Marine Chemistry, 89*(1-4), 69-88. doi: 10.1016/j.marchem.2004.02.008

Van Baalen, C., & Marler, J. (1966). Occurrence of hydrogen peroxide in sea water. *Nature, 211*(5052), 951-951. doi: 10.1038/211951a0

Voelker, B. M., Sedlak, D. L., & Zafiriou, O. C. (2000). Chemistry of superoxide radical in seawater: Reactions with organic Cu complexes. *Environmental science & technology, 34*(6), 1036-1042. doi: 10.1021/es990545x

Wuttig, K., Heller, M. I., & Croot, P. L. (2013). Pathways of superoxide (O2–) decay in the Eastern Tropical North Atlantic. *Environmental science & technology, 47*(18), 10249-10256. doi: 10.1021/es401658t

Zafiriou, O. C., Joussot-Dubien, J., Zepp, R. G., & Zika, R. G. (1984). Photochemistry of natural waters. *Environmental science & technology, 18*(12), 358A-371A.

Zepp, R., Erickson Iii, D., Paul, N., & Sulzberger, B. (2007). Interactive effects of solar UV radiation and climate change on biogeochemical cycling. *Photochemical & Photobiological Sciences, 6*(3), 286-300. doi: 10.1039/B700021A

Zepp, R. G., & Schlotzhauer, P. F. (1981). Comparison of photochemical behavior of various humic substances in water: III. Spectroscopic properties of humic substances. *Chemosphere, 10*(5), 479-486. doi: 10.1016/0045-6535(81)90148-X

Zhang, Y., & Blough, N. V. (2016). Photoproduction of one-electron reducing intermediates by chromophoric dissolved organic matter (CDOM): relation to O2–and H2O2 photoproduction and CDOM photooxidation. *Environmental science & technology, 50*(20), 11008-11015. doi: 10.1021/acs.est.6b02919

Zhang, Y., Del Vecchio, R., & Blough, N. V. (2012). Investigating the mechanism of hydrogen peroxide photoproduction by humic substances. *Environmental science & technology, 46*(21), 11836-11843. doi: 10.1021/es3029582

Zhang, Y., Zhou, L., Zhou, Y., Zhang, L., Yao, X., Shi, K., Jeppesen, E., Yu, Q., & Zhu, W. (2021). Chromophoric dissolved organic matter in inland waters: Present knowledge and future challenges. *Science of The Total Environment, 759*, 143550. doi: 10.1016/j.scitotenv.2020.143550

CHAPTER 2

ILLUMINATING SUPEROXIDE PATHWAYS IN IRRADIATED NATURAL WATERS USING VARIED CHEMICAL PARAMETERS[1]

[1]Arlinghaus, K. M. and Miller, W. L. To be submitted to *Limnology and Oceanography*.

Abstract

Superoxide (O_2^-) is a reactive oxygen species (ROS) that is primarily produced by the one-electron transfer of photo-oxidized colored dissolved organic matter (CDOM) to O_2 in sunlit natural waters. Here we examine the environmental and chemical parameters (pH, ionic strength, buffer, and halides) that may influence O_2^- photochemical decay pathways in natural water. Using the enzyme superoxide dismutase (SOD) and H_2O_2 measurements, we present results from an irradiated freshwater CDOM source indicating that O_2^- reductive decay pathways (C/C_{SOD} and P/P_{SOD}) dominate with increased pH and NaCl additions and maximal photoproduction rates (R_{O2-}) increase with carbonate compared to borate buffer. Over 2-hrs of irradiation, a significant decline in R_{O2-} and a minor increase in oxidative pathways was seen for all samples. We suggest that observed nonlinear H_2O_2 accumulation in irradiated samples is likely due to decreased electron availability to oxygen and less so to the production of photo-oxidized species.

1. Introduction

Natural surface waters are unique from underlying waters due to the presence of photochemically produced reactive oxygen species (ROS) and direct atmospheric interactions (Zafiriou et al., 1984; Kieber et al., 2003). Photoproduction of ROS results primarily from the absorption of ultraviolet radiation (UVR; 280–400 nm) by chromophoric dissolved organic matter (CDOM; Zepp & Schlotzhauer, 1981; Blough & Zepp, 1995; Clark & Zika, 2000; Sharpless & Blough, 2014). ROS are free radical molecules that are produced by redox reactions or electron excited states in oxygen. These molecules are highly reactive with a strong affinity to donate or accept another electron to achieve stability (Ho et al., 1995). ROS participate in critical

redox chemistry and have significant consequences for the biogeochemical cycling of essential trace elements and reduced carbon in the ocean (Blough & Zepp, 1995; Burns et al., 2012).

Superoxide (O_2^-) represents the initial one-electron transfer to O_2 and is the precursor for subsequent ROS formation that results from the photodegradation of CDOM (Eq. 1; Burns et al., 2012).

$$CDOM + O_2 + h\nu \rightarrow CDOM^+_{oxid} + O_2^- \quad (1)$$

Marine photochemistry, however, is not the only source of O_2^- in the ocean. Superoxide can also be produced by the redox cycling of transition metals (Burns et al., 2012), enzymatic reactions (e.g. xanthine oxidase; Bielski et al., 1985), and biological respiration of microorganisms (Sutherland et al., 2020; Hansel & Diaz, 2021).

Superoxide pathways can control the fate of O_2 by its ability to act as either a reductant (Eq. 2) or oxidant (Eq. 3) through its potential sinks (Ho et al., 1995; Goldstone and Voelker, 2000). An uncatalyzed dismutation reaction also exists for O_2^- and its conjugate acid, HO_2, in which O_2^- is reduced to form molecular O_2, H_2O_2, and OH^- (Eq. 4; Bielski et al., 1985).

Oxidation: $$O_2^- + Y_{ox} \rightarrow O_2 + Y_{red} \quad (2)$$

Reduction: $$O_2^- + X_{red} + 2H^+ \rightarrow H_2O_2 + X_{ox} \quad (3)$$

Dismutation: $$O_2^- + HO_2 + H_2O \rightarrow H_2O_2 + O_2 + OH^- \quad (4)$$

Essentially, superoxide reactions determine whether O_2 returns to the dissolved O_2 pool or continues to subsequent reductive pathways to H_2O_2 and potentially produce hydroxyl radicals (•OH) and eventually H_2O. Furthermore, extracellular O_2^- production has been suggested to be responsible for 5–19% of the sinks in the marine oxygen budget (Sutherland et al., 2020). Should superoxide reduction pathways dominate, major O_2 loss in the marine oxygen cycle would occur. This potential to direct subsequent photochemically mediated redox reactions gives O_2^- a

"gatekeeping" position in determining the ultimate electron fate, and thus, it is a key intermediate in the cycling of oxygen, organic matter, and trace metals in sunlit waters (Powers & Miller, 2016).

Superoxide production rates, however, are difficult to measure directly due to low O_2^- steady-state concentrations and rapid decay rates. Reported superoxide steady-state concentrations $[O_2^-]_{ss}$ range from 0.01–86 nM and dark decay rates vary from 0.0001–0.2 s^{-1}, though many of the O_2^- decay studies were experimentally catalyzed by trace metals (e.g. Cu, Fe, and Mn) or organic matter (outlined in Fuji and Otani, 2017). Results from these studies suggested interactions with metal compounds (Voelker et al., 2000; Heller & Croot, 2010b; Wuttig et al., 2013) and organic species with aromatic moieties (i.e. antioxidants, CDOM) such as quinones, phenols/polyphenols, or humics (Voelker et al., 2000; Heller & Croot, 2010a; Heller et al., 2016; Fujji & Otani, 2017; Ma et al., 2020) as potential abiotic sinks for O_2^- in seawater.

Superoxide decay has been further explored using the enzyme superoxide dismutase (SOD) to determine the relationship between oxidative and reductive pathways (Petasne & Zika, 1987; Shaked et al., 2010; Garg et al., 2011; Powers & Miller, 2014; Powers & Miller, 2016). Estimates of O_2^- production and decay rates were determined using 2:1 stoichiometry from measured H_2O_2 (Eq. 5; Burns et al., 2012).

$$2O_2^- + 2H^+ \xrightarrow{SOD} O_2 + H_2O_2 \quad (5)$$

Several of these studies suggest that dismutation to H_2O_2 (reductive pathway) may not always be the primary sink for O_2^-, as once assumed, and that oxidative pathways make up between 40–70% of O_2^- reactions in seawater (Petasne & Zika, 1987; Garg et al., 2011; Powers & Miller, 2016). Therefore, this 2:1 assumption for naturally occurring H_2O_2 could grossly underestimate the predicted photochemical rates of superoxide. However, this oxidative sink predominance has

not been observed across all systems. Photochemical experiments in the Gulf of Aqaba (Shaked et al., 2010) and a limited study from the Gulf of Alaska (Powers & Miller, 2014) found no effect of SOD on H_2O_2 photoproduction, thus suggesting O_2^- reduction to H_2O_2 as the dominant decay pathway.

These observations of predominant oxidative decay pathways for O_2^- are further supported by work using a single electron probe in irradiated solutions. Recent evidence has been presented showing one electron-reductants (OER) are formed during the initial photoexcitation and intramolecular electron transfer of CDOM react with dissolved O_2 to form O_2^- (Zhang et al., 2012). Two studies from this same group used a nitroxide radical probe (3AP) to determine OER photoproduction rates, and thereby, estimate O_2^- formation across standard humic and fulvic materials, as well as natural organic matter in freshwater (Zhang & Blough, 2016; Le Roux et al., 2021). Both studies proposed a significant oxidative sink for O_2^- around 65–88% that they suggest is caused by the simultaneous photoproduction of phenoxy radicals with CDOM.

In the current study, we examine environmental and chemical parameters that could control superoxide photochemical pathways by comparing H_2O_2 production with superoxide dismutase (forcing a 2:1stoichiometry) to natural samples without the enzyme. This work fills gaps in ROS redox reactions in irradiated samples by exploring O_2^- pathways in freshwater and seawater samples using H_2O_2 analysis. CDOM collected from a freshwater source served as a "standard" natural initiator of photochemical reactions that was augmented chemically to approximate specific seawater characteristics and components (ionic strength, carbonate, halides, and pH) to investigate the role of each in superoxide pathways. Superoxide dismutase (SOD) is used to infer maximal O_2^- photoproduction rates from H_2O_2 measurements and subsequent

oxidative or reductive pathways in each experimental treatment. These results provide new information on the environmental and chemical parameters with the potential to control O_2^- reaction pathways in irradiated samples and help identify further studies needed to accurately model ROS kinetics in natural waters. Furthermore, this study will deepen our understanding of the role of photochemistry in biogeochemical cycles and the redox state of sunlit waters.

2. Methods

2.1 Sample Collection and Chemical Additions

Freshwater samples were collected from Lake Herrick, Athens, GA, USA, in January 2020, July 2020, and January 2021 into a 20 L polyethylene container. Water was 0.2µm filtered immediately following collection and stored at 4°C until used for irradiations. Using freshwater provides a natural source of organic material for repeated photochemical experiments that allows investigation of individual chemical constituents of sea water from a freshwater starting point. Chemical additions (**Table 1**) to this CDOM source were performed to build "seawater-like" solutions with controlled characteristics having potential to alter photochemical pathways in marine waters (ionic strength, buffer, halides, and pH). The influence of iron was also examined by adding fluoride to block its participation in photochemical reactions (Gao & Zepp, 1998).

2.2 H_2O_2 Analysis

Hydrogen peroxide was measured using a flow injection chemiluminescent detection system (Waterville Analytical; King et al., 2007) that employed 2 µM 10-methyl-9-(p-formylphenyl)-acridinium carboxylate trifluoromethanesulfonate (AE; provided by Dr. James J. Kiddle, Western Michigan University). Samples were injected into a Teflon sample loop (VICI

10-port valve), transported by peristaltic pump (Rainin) and mixed with buffer and AE in a Teflon chemiluminescent flow cell (Global FIA, Inc.) located in front of a photomultiplier tube (PMT; Hamamatsu HC135 PMT, 900 V, 400 ms integration). Standards were made prior to every analysis in the specific experimental solution being irradiated using dilutions from a stock solution of 30% H_2O_2 (J. T. Baker). The concentration of this stock solution was determined using UV-Vis spectroscopy (Aqualog, Horiba Scientific) with MQ as the absorbance blank (molar absorptivity 38.1 M^{-1} cm^{-1} at 240nm; Miller & Kester, 1988). Average H_2O_2 concentrations (nM) were calculated from integrated mV peak areas (Labview, Waterville Analytical) of three or more replicate sample injections using a linear equation from standard additions. The H_2O_2 detection limit for this FIA chemiluminescent system is 2 nM (Powers & Miller, 2016).

2.3 Photochemical Experiments

Solutions (300 mL) were stirred in two temperature-controlled jacketed beakers covered with quartz glass and irradiated side by side using a Suntest CPS solar simulator equipped with a 1.5 kW xenon lamp (Atlas) fitted with IR-filtering window glass that simulates sunlight reaching the earth's surface (290–800 nm; **Figure S1**). Before and after irradiation, all solutions were analyzed by UV-Vis spectroscopy to determine the CDOM spectral absorption (m^{-1}):

$$a(\lambda) = 2.303\ A(\lambda)/r \qquad (6)$$

where $a(\lambda)$ is the absorption coefficient at wavelengths λ and A is the absorbance in a spectrophotometer with pathlength, r, in meters (Blough et al., 1997; Clark & Zika, 2000; Twardowski et al., 2004). All subsequent photochemical rate data was normalized to total photon absorption; dividing by the measured integrated absorption from 290 to 400 nm ($a_{(290–400)}$) of pre-

irradiated solutions to allow direct comparison of photochemical reaction rates for solutions with different CDOM spectra. This corrects for initial CDOM absorbance and any subsequent affects to absorbance from chemical modifications to our samples. However, $a_{(290–400)}$ does not include photobleaching since it was calculated from solutions prior to irradiation (t=0).

For each experimental irradiation, one beaker was treated with 2000 U/L SOD (S5395-30KU, Sigma) immediately prior to irradiation while the other beaker contained no SOD. Higher concentrations of SOD resulted in identical H_2O_2 accumulation in irradiated samples, allowing the assumption to be made that O_2^- is quantitively catalyzed to H_2O_2 by SOD in our irradiations. Stock solutions of 1.2 x 10^6 U/L SOD (calculated from the manufacturer's reported activity) were prepared in 500 µL Milli-Q (Millipore) aliquots and stored at –20°C prior to experiments. Samples were analyzed for hydrogen peroxide at 15-minute intervals during a 2-hour irradiation to determine accumulation rates with and without SOD treatments.

2.4 Ratio and Rate Determination

A concentration ratio (C/C_{SOD}; Eq. 7) was calculated by dividing the H_2O_2 concentration (nM) in untreated samples by the H_2O_2 concentrations in the SOD treated samples at 60 and 120 minutes of irradiation. A production rate ratio (P/P_{SOD}; Eq. 8) was calculated by dividing the H_2O_2 photo-accumulation rate in untreated samples by the H_2O_2 photo-accumulation rate in treated SOD samples over two irradiation time intervals: initial (0–60 min) and final (60–120 min).

$$C/C_{SOD} = \frac{[H2O2]_{NoSOD}}{[H2O2]_{SOD}} \quad (7)$$

$$P/P_{SOD} = \frac{\Delta\,[H2O2]_{NoSOD}}{\Delta time} \Big/ \frac{\Delta\,[H2O2]_{SOD}}{\Delta time} \quad (8)$$

$$R_{O2-} = 2 \cdot \frac{\Delta\,[H2O2]_{SOD}}{\Delta time} \Big/ a_{(290-400)} \quad (9)$$

These quantitative ratios can then be used to calculate the percentage of superoxide that proceeds via oxidative and reductive pathways in each solution using the assumption that SOD treatment results in 100% conversion to H_2O_2 via dismutation. For example, a ratio of 0.8 indicates that 80% of the O_2^- produced during irradiation is reduced to H_2O_2 and 20% is lost through an alternative oxidative pathway, likely back to molecular oxygen. These ratios are useful proxies because they are not subject to CDOM absorption variability across samples since the calculation is a direct comparison of the same DOM for each experiment. However, they do not represent percentages of O_2 removed from the marine oxygen budget in natural aquatic systems. Rather, they indicate the percent reduction of O_2^- relative to catalyzed dismutation in our experiments. Lastly, maximum O_2^- photoproduction rates (R_{O2-}; nM x m / min) were calculated over specified 30-min intervals by assuming a 2:1 superoxide dismutation ratio in the SOD treated samples. As in all rate determinations, these were normalized to CDOM (m^{-1}) (Eq. 9).

2.5 Data Analysis

Data representation and statistical analysis for rates and ratios were determined in R-Studio (R Core Team, 2020). Box and whisker plots were created based on defined variable groups and demonstrate the median, interquartile range (IQR), and minimum/maximum data points without outliers. Outliers were defined as being more than 1.5 times the IQR. Our data for P/P_{SOD} was the most variable data set, resulting in outliers that significantly skewed the calculated mean values (**Figure S2a**). Therefore, statistical outliers were removed to reveal the trends and constrain the limits of our P/P_{SOD} data (**Figure S2b**). Outliers were not removed from our C/C_{SOD} and R_{O2-} data.

T-tests across variable groups were performed in R to generate estimates of mean difference and compare the central tendency of ratios and rates. Pearson correlation coefficients were also determined in R to measure the strength of the linear relationship between two variables. Additionally, a multiple regression with backward elimination was executed in R to find the most appropriate model and compare the effect strength of each variable (time, absorption integral, NaCl, borate, carbonate, Br^-, I^-) on C/C_{SOD}, P/P_{SOD}, and R_{O2-}.

3. Results

3.1 Validation of Photon Absorbance and SOD Quenching

To confirm that both the SOD-treated and untreated samples were receiving the same photon energy from the solar simulator, an initial experiment was performed to compare the H_2O_2 production in beakers containing filtered freshwater DOM with no chemical additions and no SOD during a 2-hour irradiation. The only variable in this initial experiment was beaker position under the solar simulator (left or right). The mean difference between the two beakers was calculated from the average H_2O_2 concentration at each 15-minute interval. H_2O_2 increased from ~300 to 900 nM over the 2-hr irradiation. The average difference in mean H_2O_2 photoproduction for all time points was 6.2 ± 45 nM and was not statistically significant (t=0.41, df=8, p=0.69) as shown in **Figure S3**. Therefore, we approached all subsequent experiments with the assumption that the SOD treated (left) and untreated (right) beakers are receiving the same photon energy from the solar simulator within statistical error, and that this does not contribute to measured variability in H_2O_2 accumulation seen in subsequent +/– SOD experiments.

SOD concentrations were investigated to confirm that photochemically generated O_2^- was quantitatively catalyzed by SOD to proceed down the reductive pathway to H_2O_2. Published

results in similar irradiations report that 3000 U/L SOD achieves maximal H_2O_2 production (Powers & Miller., 2016). We further investigated this concentration by measuring H_2O_2 production during 2 hours of irradiation with 2000 U/L SOD and 4000 U/L SOD and found that doubling the SOD concentration does not enhance H_2O_2 accumulation within analytical uncertainty (**Figure S4**). Therefore, we can assume SOD, when added at 2000 U/L across the range of environmental parameters produced here, gives maximal H_2O_2 production with no change in structure or loss of function occurring in SOD due to extended irradiation. Direct measurements of O_2^- confirmed SOD activity for 60 minutes of exposure at maximum output under the same Suntest CPS solar simulator setup that was used in the present study (Powers & Miller, 2014; Powers et al., 2015). While we have no direct measurements of O_2^-, our data does not suggest a loss of full SOD activity with continued irradiation from 60 to 120 minutes.

3.2 CDOM Consideration

Freshwater DOM was used in these experiments to provide a natural source of organic material that has photochemical potential without the chemical constituents of seawater. However, three different collections were needed to complete the study and this likely affected the photon absorbance of samples collected from different seasons. In fact, an ANOVA showed that mean absorption integral, $a_{(290–400)}$, was statistically different for different collections (df=2 , F=201, $p<10^{-16}$; **Figure 1a**). Therefore, to make direct comparison of all photoproduction rates, it was necessary to normalize between samples to account for slightly different UV optical characteristics and $a_{(290–400)}$. This correction, however, does not include photobleaching since it was performed with $a_{(290–400)}$ obtained before any irradiation (t=0). Photochemical fading in each sample was determined following the 2-hour irradiation using the integrated CDOM absorption

coefficient from 290–400 nm as noted in the methods (**Table S1**). The average fading of $a_{(290–400)}$ over all samples was 5.6 ± 5.7%. Any loss in photochemical production rates larger than 6% over the 2-hr irradiation is assumed not to result from CDOM fading.

In addition to CDOM absorbance differences, potential changes in the photoreactivity for seasonal samples were also examined. Using CDOM normalized ratios pooled for all samples of both 0–60 and 60–120 minute irradiation time periods, neither C/C_{SOD} nor P/P_{SOD} were significantly correlated to CDOM (i.e. $a_{(290–400)}$; **Figure S5a&b**). CDOM absorption, did however, identify a slightly significant, positive correlation when applied to the maximum O_2^- production rate (R_{O2-}) over the 30–60 (r=0.49, p=0.003) and 60–90 (r=0.42, p=0.019) minute irradiation intervals. There was no such correlation for any other time intervals (**Figure S5c**).

Furthermore, altered photochemical rates among experimental solutions may result directly from changes in $a_{(290–400)}$ created by various chemical additions. Shifts in CDOM spectra due to pH changes are well-known. A Pearson's correlation coefficient test in R was used to determine the strength of the relationship between $a_{(290–400)}$ and pH for each collection season (**Figure 1b**). Absorption integral and pH had a positive, statistically non-zero correlation for all collection seasons. Correlations were greater for solutions made from the June 2020 (r=0.72, p=0.638) and January 2021 (r=0.79, p=0.003) collections than from the January 2020 collections (r=0.36, p<0.001).

3.3 Effect of pH

Not only does pH affect the CDOM spectra, but it can also influence the O_2^- pathways directly. Both C/C_{SOD} and P/P_{SOD} ratios across all chemically augmented solutions had a significant positively correlations to pH that continued with irradiation (**Figure 2a&b**). R_{O2-},

however, was not correlated to pH, except over the 60–90 min time interval (r=0.36, p=0.045). This is likely a result of our normalization to $a_{(290–400)}$ which accounts for chemical effects on the absorption of CDOM, one which we observed with pH. Since pH clearly alters both $a_{(290–400)}$ and ratios, further more detailed data analysis will focus on experiments using either solutions at natural freshwater pH (6.6–7.6) or at a pH that more closely approximate seawater (>7.6).

3.4 NaCl Additions

NaCl additions had a strong effect on C/C_{SOD} and P/P_{SOD} with mean values significantly higher from those of untreated freshwater solutions (**Table S2a & b**). This increase was evident at both 60-min (p=0.001) and 120-min (p=0.021) for C/C_{SOD} (**Figure 3**). While this increase was also observed during the first hour, 0–60 min, of irradiation for P/P_{SOD} (p=0.016), statistical analysis for P/P_{SOD} during the final hour, 60–120 min, was not possible because of insufficient data resulting from removal of outliers (**Figure 4, Table S2b**). In contrast, the addition of NaCl to our samples did not statistically change R_{O2-}, though the mean R_{O2-} was slightly lower for NaCl solutions over each time interval (**Figure 5, Table S2c**).

3.5 Borate and Carbonate Buffers

The difference in borate and carbonate buffers was also investigated. The mean difference between borate and carbonate buffers was not significant for C/C_{SOD} and P/P_{SOD} (**Figures 3 & 4, Table S2a & b,**). However, there was a statistical difference in R_{O2-} between borate and carbonate buffers at a similar pH during the initial hour of irradiation (**Figure 5, Table S2c**).

3.6 NaBr and NaI Additions

Halide experiments were built from freshwater solutions with added NaCl and carbonate buffer to adjust the sample pH ≥ 7.6. Therefore, results from these experiments are in reference to these "seawater-like" solutions. Additions of bromide (Br^-) and iodide (I^-) did not demonstrate clearly consistent results and consequently showed limited statistical changes. This is largely due to the small sample size. However, we can observe a few marginal trends across the data. The addition of NaI to carbonate buffered NaCl solutions showed increased C/C_{SOD} and P/P_{SOD} ($p=0.099$) during the first hour of irradiation relative to samples with no I^-, though this was only statistically significant for C/C_{SOD} ($p=0.26$; **Figure 3 & 4, Table S2a&b**). Interestingly, P/P_{SOD} slightly decreased with I^- during the second hour of irradiation. In contrast, the addition of NaBr showed a slight decrease in both C/C_{SOD} ($p=0.243$) and P/P_{SOD} ($p=0.265$) during the first hour of irradiation. Solutions with both Br^- and I^- added together did not significantly change from the mean C/C_{SOD} values of solutions with no halide additions. However, there was a slight decline of P/P_{SOD} during the final hour of irradiation ($p=0.175$).

R_{O2^-} showed no statistical difference for all halide addition across all irradiation intervals, except in solutions with both Br^- and I^- where R_{O2^-} was significantly different from the carbonate buffered NaCl solutions without halides over the 30–60 min irradiation interval (**Figure 5, Table S2c**). There was, however, a small decrease in R_{O2^-} with halides seen during the first 90 minutes of irradiation. Ultimately, the effect of halide additions on C/C_{SOD}, P/P_{SOD}, and R_{O2^-} is largely inconclusive due to small data sets and the absence of any consistent trends in relationships across irradiation intervals.

3.7 Effect of Continued Irradiation

For almost all solutions, C/C_{SOD} and P/P_{SOD} showed no statistical change over 2-hrs of irradiation (**Figure 6a&b, Table 2a&b**). However, most solutions slightly declined over time with some variation across chemical additions. The only significant decrease in C/C_{SOD} ratios over time was for the borate buffered NaCl solutions ($p=0.040$). Additionally, the only significant decrease in P/P_{SOD} over time was for the carbonate buffer NaCl solutions with NaI ($p=0.046$).

The most notable observed trend over our 2-hours of irradiation was the decreasing rate of maximum superoxide photoproduction across all chemical variations ($r=-0.69$, $p<10^{-16}$; **Figure 6c**). A notable negative correlation with time was evident for all solutions, with statistical significance for all except the borate additions (**Figure 5**, **Table 2c**).

4. Discussion

4.1 CDOM Photoreactivity

The differences in CDOM between different times of collection may be attributed to seasonal variability in meteorological and hydrological processes such as photobleaching, precipitation, and inflow runoff which largely control CDOM abundance and composition (**Figure 1a**; Coble, 2008; Zhang et al., 2021). The resulting CDOM characteristics of our Lake Herrick samples reflect local sources and the short-term balance of these sources with their sinks. The 38% lower $a_{(290-400)}$ seen in our summer collection may represent an increased CDOM sink due to photochemical fading, a decrease in precipitation (and resulting contribution from the watershed), or both. Given that summer drought conditions have been shown to decrease absorptivity at 320 nm in remote Nova Scotia lakes by as much as 80% (Moore, 1999), the

differences seen here are well within the possible range generated by change in rainfall and fading.

Ionic strength and pH can alter CDOM structural conformation with subsequent changes in optical properties and potential for electron transfer (Lu et al., 2015). Specifically, DOM polymers and colloids condense at low pH and high ionic strength, limiting absorption abilities of chromophores. In contrast, DOM expands at higher pH and lower ionic strength, resulting in greater initial light absorption (Spencer et al., 2007; Pace et al., 2012; Lu et al., 2015). Similarly, the integrated CDOM absorption ($a_{(290–400)}$) in our samples was generally highest when raised to a pH of 8 (**Figure 1b**). This $a_{(290–400)}$ shift represents an increase in photon absorption and potential for a direct increase in photochemical production rates. Consequently, to examine the role of varied chemical parameters without inclusion of confounding optical changes, we normalized our results to CDOM as described above.

This procedure does not, however, correct any variations in overall CDOM "photochemical efficiency", defined as product per photon absorbed, that results from differences in source material, exposure history, or conformational changes. In other words, once corrected to equivalent photon absorption, samples from different seasons and with differing pH values can also differ in their capacity for the photoproduction of H_2O_2 and O_2^-. Therefore, pooling all data across collection seasons and all treatments admittedly may create more variability. The C/C_{SOD} and P/P_{SOD} ratios are less likely to include this variability since they directly compare photoproduction from solutions with identical CDOM irradiated side by side. It is possible, however, that variations in the oxidative and reductive pathways captured by these ratios does reflect variations in the reactivity of the DOM source material beyond simple optics.

Once normalized to CDOM, R_{O2-} would reveal differences across samples due to variability in CDOM photochemical efficiency since it quantifies O_2^- production directly.

Furthermore, it would be remiss not to acknowledge our use of freshwater DOM in a study aimed at understanding seawater ROS chemistry. Freshwater and seawater DOM are inherently different in their source, and therefore, also their photochemical characteristics. For example, freshwater DOM often originates from terrestrial organics such as vascular plant debris resulting in an enrichment of lignin-derived polyphenols. Algae-derived marine DOM in the open ocean, in comparison, predominantly lacks these compounds (Meyers-Schulte & Hedges, 1986; Opsahl & Banner, 1997). Furthermore, past studies have determined marine DOM to generally have a lower abundance of oxygen-rich molecules (Koch et al., 2005; Sleight & Hatcher, 2008). These molecular differences between freshwater and seawater DOM could influence CDOM photochemical efficiency. Additional studies with DOM extracted from known marine organics used as photochemical source for controlled studies like the one presented here (pH, ionic strength, carbonate, halogens, etc.) may reveal differences between marine and freshwater DOM with regard to ROS redox pathways and photoreactivity. Thus, extrapolation of the environmental and chemical controls on superoxide pathways examined in this study would require additional study of marine-derived DOM to better predict rates of superoxide production and decay in open ocean systems.

4.2 Effect of pH and Ionic Strength

As illustrated in **Figures 2a & b**, a significant positive correlation exists between our ratio values and pH. The C/C_{SOD} and P/P_{SOD} correlation with pH suggests that O_2^- likely participates in fewer oxidative pathways at a pH of 8 than it does at lower pH. The most obvious

explanation of this correlation may, at first glance, appear related to the acid-base chemistry of superoxide with O_2^- and its conjugate acid, perhydroxyl radical (HO_2), having a pKa of 4.8 in aqueous solution (Bielski et al., 1985). The observed rate (k_{obs}) of the disproportionation reaction (Eq. 8) is described at pH values above 6 as follows (Bielski et al., 1985),

$$k_{obs} = 6 \times 10^{12} [H^+] \text{ L mol}^{-1} \text{ s}^{-1} \quad (8)$$

indicating that production of H_2O_2 from uncatalyzed dismutation of superoxide at pH 6 should be 100-times faster than at pH 8, approaching ratios of 1 when compared to SOD treatments that force this same reductive dismutation. We find an opposite trend, suggesting that even with this kinetic advantage for dismutation at low pH, oxidative pathways remain kinetically favored overall. These oxidative pathways may result from the acid-base chemistry of CDOM or trace metals within our samples. Fujii and Ontani (2017) observed slightly increased H_2O_2 production rates from pH 6 to 8 with humic substances and suggest humic substance catalyzed superoxide decay is likely influenced by pH changes. These results support our observations since they suggest reductive pathways toward H_2O_2 dominate at a pH of 8. Therefore, acid-base chemistry of the organic substances that make up CDOM are likely a significant influence for superoxide decay pathways.

The general absence of correlations between R_{O2-} and pH, with the single exception being the 60–90 min interval (**Figure 2c**), suggests pH driven changes in CDOM absorption were the primary source of any variations in superoxide production, and that normalization with $a_{(290–400)}$ essentially removed this effect. Despite data variability and lack of statistical significance across all samples, CDOM acid-base chemistry could influence electron availability and distribution within the CDOM pool. For example, phenols are deprotonated at higher pHs resulting in more accessible redox-active groups and potentially making CDOM more likely to donate an electron

to O_2 to produce O_2^- (Lu et al., 2015). Therefore, pH variability in natural waters could influence superoxide photoproduction rates, though we do not see statistically significant correlation in our samples.

The ionic strength for our NaCl additions matched that of full-strength seawater (**Table 1**). While this gives the solutions equivalent total charge density, it may have missed some superoxide dynamics present in authentic seawater. A recent study, similar to the superoxide pathway analysis presented here, quantified photoproduction rates of one electron-reductants (OER; R_H) and H_2O_2 (R_{H2O2}) in freshwater solutions with 50mM borate buffer at pH 8 with NaCl and Sigma-Aldrich "sea salt" additions at concentrations of 18 and 28 ppt (Le Roux et al., 2021). They observed a decrease in oxidative pathways (represented as R_H/ R_{H2O2}) with both NaCl and "sea salt" additions. This is consistent with the decrease in oxidative pathways we saw for C/C_{SOD} and P/P_{SOD} with NaCl additions. As shown in **Fig. 3b and 4b**, both C/C_{SOD} and P/P_{SOD} increased markedly with NaCl additions. Therefore, it is possible oxidative pathways decline and reductive pathways to H_2O_2 dominate with increased ionic strength.

Additionally, we observed a small decrease in R_{O2-} with NaCl additions (**Figure 5b**). Le Roux et al. (2021) saw a similar trend in R_H with "sea salt", but not with NaCl. This negative correlation was also seen in irradiated eastern Caribbean waters where O_2^- production rates slowed with increased salinity (Micinski et al., 1993). It is unclear why photoproduction rates for OER and superoxide would decrease with NaCl, "sea salt", or natural salinity gradients. Perhaps, ionic interactions interfere with electron availability. Lu et al. (2015) observed decreased electron-transfer capacity of DOM with increased ionic strength. Overall, the general observations from these studies suggest there is more to learn about the controls of ionic strength on the rates of photoproduction for OER and superoxide.

The environmental relevance of pH and ionic strength in natural water continues to be a heavily researched topic, especially in coastal ecosystems where the transition from freshwater to saltwater chemistry creates strong pH and salinity gradients. The relationships presented in this study may help elucidate superoxide pathways in real coastal systems when paired with field measurements. In a transect from inshore to oligotrophic waters in the South Atlantic Bight (SAB) during the summer of 2016, Powers and Miller (2016) observed a relationship between salinity and redox partitioning of O_2^- pathways that was opposite the one seen here. Their results showed the highest O_2^- : H_2O_2 photoproduction ratio (equivalent to our P/P_{SOD} from 0–60 min) in clear waters of the Gulf Stream which suggests oxidative O_2^- decay pathways increase relative to reductive pathways with decreased CDOM absorbance and increased salinity. In coastal environments, the ionic strength increases rapidly from freshwater rivers water to brackish estuaries and marshes to salty seawater; thus, a deeper understanding of how superoxide redox pathways change across diverse aquatic environments will require specific studies directed at these sharp gradients.

4.3 Carbonate Interactions

The acid-base chemistry of carbonic acid is the dominant buffering system in oxygenated natural waters and has the potential to participate in photochemistry. Carbonate radicals ($CO_3^{\bullet-}$) are formed during the reaction of photogenerated hydroxyl radicals (•OH) and carbonate/bicarbonate anions (CO_3^{2-}/ HCO_3^-; Vione et al., 2014; Yan et al., 2019). Borate buffer has long been used in photochemical studies to bypass this potential for photochemical influences. For this reason, the difference in borate and carbonate buffers was investigated. Similarity of results in carbonate and borate buffer would support the conclusion that carbonate

also does not participate in photochemistry in our experiments. Since the mean difference of borate and carbonate solutions with NaCl were within statistical error of each other for C/C_{SOD} and P/P_{SOD} (**Figures 3 & 4**), we can assume carbonate chemistry is not changing O_2^-decay pathways in our samples.

Carbonate buffered NaCl solutions, however, resulted in significantly faster R_{O2-} compared to borate buffer NaCl solutions during the initial hour of irradiation (**Figure 5**). Interactions with $CO_3^{\bullet-}$ could potentially be responsible for this observation. A study by Yan et al. (2019) saw enhanced photobleaching of CDOM in the presence of CO_3^{2-}/ HCO_3^-. They attribute this increased loss of CDOM absorbance to the photogeneration of $CO_3^{\bullet-}$ and its ability to alter the phenolic moieties. This suggests $CO_3^{\bullet-}$ is actively participating in photochemical reactions and could potentially contribute to enhanced R_{O2-} in short-term irradiations. Long-term UV-exposure, however, would likely result in decreased R_{O2-} in the presence of carbonate buffer due to enhanced photobleaching. Perhaps, faster fading in carbonate buffered NaCl solutions explains the large drop in R_{O2-} near the end of our 2-hr irradiation resulting in similar rates for carbonate and borate solutions over the last 30 minutes of irradiation (**Figure 5**). Additionally, the effects of carbonate buffers on indirect photodegradation of antibiotics were recently investigated (Tang et al., 2021). Opposite trends with controlled concentration gradients of HCO_3^- were observed with two antibiotics, sulfathiazole (ST) and sulfamerazine (SM), in augmented pure water solutions with salinity 30‰ and pH = 8. ST had a clear enhancement of photodegradation as [HCO_3^-] increased while SM had reduced photodegradation with increased [HCO_3^-]. Altogether, this suggests that the presence of much higher carbonate concentrations in seawater relative to freshwater adds a layer of complexity in determining ROS production and decay rates.

4.4 Halide Photochemistry

Halides can be reduced by photochemical reactions in natural water to produce halogen radicals and reactive halogen species (RHS). These radicals occur either through direct reduction by photo-oxidized DOM or indirectly by photogenerated ROS (Yang & Pignatello, 2017; Dong et al., 2021). Additionally, halogens may be incorporated into the bulk DOM pool during UV solar radiation creating organohalogen compounds that may also be photolabile (Mendez-Diaz, et al. 2014; Yang & Pignatello, 2017; Dong et al., 2021). For this reason, halides and their radical/reactive forms have the potential to interact with ROS cycling in sunlit surface waters. To date, there are no studies that directly investigate $[O_2^{-}]ss$ or decay rates under halide-controlled experiments. Most previous work with halide photochemistry has focused on reactions with DOM (specifically triplet excited states, $^3DOM^*$), hydroxyl radical (•OH), and singlet oxygen ($^1O_2$) (Mopper & Zhou, 1990; Grebel et al., 2009; Glover & Rosario-Ortiz, 2013; Parker & Mitch, 2016)

While the limited halide additions done in the present study are largely statistically inconclusive, C/C_{SOD}, P/P_{SOD}, and R_{O2-} do seem to decrease slightly when NaBr is added to carbonate buffered NaCl solutions during the initial hour of irradiation (**Figures 3, 4, and 5**). In contrast, C/C_{SOD}, and P/P_{SOD} ratios increase slightly during the initial hour of irradiation when NaI alone is added to carbonate buffered NaCl solutions. The second hour of irradiation, however, trends amongst halide groups are difficult to distinguish due to excessive variability. The halide additions to carbonate buffered NaCl solutions are our most similar samples to the chemical composition of seawater. The differences observed over various irradiation intervals might reflect a changing halide photochemical participation in ROS photochemistry as solar exposure continues but our data cannot provide strong support for this possibility.

Bromide is one of the most abundant halides in the ocean, after Cl^-, with concentrations around 0.8 mM (Yang & Pignatello, 2017). The small reduction seen in C/C_{SOD} and P/P_{SOD} ratios during the first hour of irradiation for solutions with NaBr (**Figure 3e & 4e**) may indicate the addition of oxidative pathways by bromide (and presumably production of a reactive Br species) in sunlit natural waters. Bromide in seawater is an effective •OH scavenger. In fact, it is the primary scavenger of •OH production in surface waters (Mopper & Zhou, 1990; Vione et al., 2014), quantitatively forming a dibromide radical, $•Br_2^-$, in the process which then reacts with carbonate species in seawater (Zafiriou et al., 1987; Dong et al., 2021). We cannot, however, draw a direct correlation with our limited data between these radical reactions and superoxide pathways. Furthermore, studies have determined that Cl^- and Br^- in seawater are responsible for increased photobleaching of CDOM (Grebel et al., 2009; Parker & Mitch 2016; Zhang et al., 2019). It is possible that enhanced photobleaching in the presence of Br^- could explain the small decrease in R_{O2-} since this rate is normalized using pre-irradiated (t=0) CDOM values. This seems unlikely, however, due to low fading seen in our samples as well as this observed rate decrease only occurring during the first hour or irradiation. There are multiple other complex reactions with Br^- in natural waters (outlined in Dong et al., 2021) that, upon further work, could explain Br^- influence on O_2^- rates and pathways.

The effect of iodide on photochemical processes in seawater has been studied less frequently in seawater, largely due its low concentrations (100–200 nM) and the fact that the primary form of iodine in the ocean is iodate (IO_3^-) (Barkley & Thompson, 1960; Yang & Pignatello, 2017). Iodide is, however, also an important scavenger of •OH in seawater (Mopper & Zhou, 1990) and can enhance methyl iodide production in irradiated filtered seawater (Moore & Zafiriou, 1994). Most recent halide studies that include reactions of iodide and its radical

forms focus on air-sea exchange, the sea surface microlayer, and the marine boundary layer (Jammoul et al., 2009; Jiao et al., 2022). We cannot make direct correlations between the available literature of I^- reactions and superoxide pathways with our limited data. Perhaps, the decrease in oxidative pathways during the first hour of irradiation (**Figure 3f & 4f**) and slightly slower R_{O2-} (**Figure 5f**) seen with NaI additions result from complex reactions involving I^- and its subsequent photochemical products. However, C/C_{SOD} and P/P_{SOD} ratios with NaI additions larger than 1 lie outside the boundaries of our experimental assumptions. It is possible, therefore, that the addition of NaI or subsequent photochemical products interfere with our chemiluminescent method but this was not examined.

4.5 Possible Photochemical O_2^- and H_2O_2 Sinks

In virtually all experiments, C/C_{SOD}, P/P_{SOD}, and R_{O2-} decreased as irradiation proceeded (**Table 2a,b,c**). The most significant and striking decrease was evident in the R_{O2-} data, showing an average decrease of 73% between the initial production rate (0–30 min) and the final rate (90–120 min) during the 2-hour irradiations for all samples (**Figure 6c**). This loss of superoxide photoproduction is consistent with published data on the time course of superoxide steady-state concentrations, $[O_2^-]ss$, in various irradiated waters. Powers et al. (2015) observed decreasing $[O_2^-]ss$ over 12 hours of continuous simulated solar irradiation in oligotrophic waters from the Gulf of Alaska. Fujii and Otani (2017) also reported a gradual decrease of O_2^- concentrations during 6 hrs of irradiation in NaCl solutions with humic substances.

The nonlinear accumulation of H_2O_2 over irradiation noted in almost all experiments may be explained by a) a loss of source, b) a H_2O_2 sink in sunlit waters, or c) both. The loss of CDOM due to photochemical fading was considered as an explanation for the decrease in ROS

source but, with an average 5.6 ± 5.7% decrease of CDOM (**Table S1**) over 2 hours of irradiation for all samples, it is clear that fading cannot fully account for this observed decrease in R_{O2-}. Since our R_{O2-} is not a direct O_2^- measurement and is instead based on an assumed $2O_2^-$:$1H_2O_2$ ratio, we must also consider O_2^- as a source for H_2O_2 accumulation. Shifts to oxidative pathways could be a potential sink for O_2^-. However, that is not consistent with the overall trends we saw for C/C_{SOD} and P/P_{SOD}. The decrease observed in these ratios during irradiation was not statistically significant suggesting the proportion of redox decay pathways for O_2^- remains relatively consistent within 2 hours of irradiation (**Figure 6a&b, Table 2a&b**). We suspect the most likely loss of O_2^- production resulting in nonlinear accumulation of H_2O_2 is decreased electron availability to oxygen. As irradiation continues, it is possible that a pool of one-electron reductants within CDOM ($CDOM^{+/-}$) builds up to compete with O_2 for electron transfer (Zhang et al., 2012; Zhang et al., 2016; Le Roux et al., 2021). This competition would result in decreased O_2^- production, and subsequently, a nonlinear accumulation of H_2O_2 over time as we see in our results.

Possible H_2O_2 sinks by direct photolysis and/or loss due to reactions with other photochemically produced oxidants could also affect our R_{O2-} calculation with SOD stoichiometry and be responsible for the non-linear accumulation seen in out filtered samples. A study by Moffet & Zafiriou (1993) in the Eastern Caribbean and Orinoco River used ^{18}O labeled H_2O_2 to determine photochemical decomposition patterns of H_2O_2. They concluded H_2O_2 photochemical decomposition rates, either by photolysis or reduction, only account for ~5% of production rates. Thus, H_2O_2 decomposition is not a major contributor to our observed decrease in R_{O2-} during irradiation. This ~5% relative loss of H_2O_2 formation, however, does suggest our 2:1 stoichiometry assumption could underestimate R_{O2-}. Since we double H_2O_2 production to

calculate R_{O2-}, a 5% photolysis rate would mean we are underestimating R_{O2-} by 10% (2 x 5%). With photolysis included, a ratio of 2.1:1 would be more accurate when calculating R_{O2-} from H_2O_2 production with SOD.

While not statistically significant, C/C_{SOD} and P/P_{SOD} ratios for most samples exhibited a slight decrease with irradiation time, indicating a relative increase in oxidative pathways with continued exposure to solar radiation (**Figure 6a&b, Table 2a&b**). As discussed above, this slight enhancement in oxidative pathways is likely not responsible for the nonlinear accumulation of H_2O_2 seen in our irradiation experiments. Nevertheless, this trend suggests small changes to O_2^- redox pathways occur during irradiation. This minute shift to oxidative pathways could be attributed to a photochemically produced transient pathway for oxidation of O_2^- as suggested in other studies (Zhang et al., 2012; King et al., 2016; Powers & Miller, 2016; Zhang et al., 2016; Ma et al., 2020).

Several different photo-activated transient species might explain this observed photochemically generated superoxide sink in seawater. Copper (Voelker et al., 2000; Heller & Croot, 2010b), manganese (Wuttig et al, 2013), and CDOM (Heller & Croot, 2010a; Heller et al., 2016) have been previously proposed as dominant pathways for O_2^- decay. Since we did not explore the role of metals in our exposures directly, this remains a possible mechanism to alter oxidative pathways. If CDOM provides an oxidative decay pathway in our experiments, it would be consistent with several other studies that suggest the accumulation of photo-oxidized CDOM ($CDOM^+$) as a prominent photo-activated oxidative sink for O_2^- (Garg et al., 2011; Zhang et al., 2012; Heller et al., 2016; Ma et al., 2020).

Further work is needed to characterize these photo-active sinks for superoxide and their specific pathways in sunlit natural waters. To date, superoxide decay rates have been determined

post-irradiation, and therefore, may not account for any additional losses by a photochemically produced transient species (Powers & Miller, 2016). Recently, interest has grown in quantifying this elusive oxidative sink. A study by King et al. (2016) presented an analytical method to estimate O_2^- antioxidant activity in naturals waters. Working in the South Atlantic, they observed 0.1–0.4 nM of "antioxidants" in surface seawater samples collected during the day with a half-life of 3–7 min in the dark, consistent with photo-reactive species capable of scavenging superoxide. Though this method does not identify the antioxidant species in their samples, the authors allude to photochemically activated organic species as a potential source for this effective "antioxidant" activity.

4.6 Conclusion

Overall, understanding the ratios and rates presented here can help us distinguish potential superoxide decay pathways and how seawater chemical parameters may influence those pathways in sunlit natural water. The results indicate that oxidative pathways, as represented by C/C_{SOD} and P/P_{SOD}, decrease with increased pH and NaCl additions. Results from halide additions, however, were largely inconclusive although Br^- and I^- did show a slight decrease and increase respectively for C/C_{SOD} and P/P_{SOD} calculated over the first hour of irradiation. In contrast, the most notable change with chemical modifications for R_{O2-} was addition of carbonate buffer, suggesting the potentially complex role of carbonate radical in the photochemical cycling of ROS in surface seawater.

The most striking trend observed across all our data was the significant decline in R_{O2-} along with a minor increase in oxidative pathways with 2 hours of continuous irradiation. We suggest that the nonlinear accumulation of H_2O_2 in sunlit waters is most likely due to decreased

electron availability to oxygen as a result of competition with photochemically produced one-electron reductants within CDOM ($CDOM^{+/-}$). Furthermore, our calculated R_{O2-} may underestimate O_2^- production rates by as much as 10% due to possible H_2O_2 photodecomposition. Altogether, the results presented in this study imply there are shifts in O_2^- decay pathways and production rates that seem to vary across natural water environments and as a function of irradiation history. This work will help predict processes that control superoxide redox reactions and fate of oxygen in natural waters, especially during solar irradiation, to improve the accuracy of photoproduction estimates and photochemical cycling models.

Tables and Figures

Table 1. Concentrations of seawater chemical additions to freshwater.

Seawater chemical parameters	Concentrations	Manufacturer
Ionic Strength	0.6M of NaCl, extra pure	Acros Organics
Buffering Capacity	Borate: 1.3–2.0 mM	Fisher Scientific
	Na□B□O□(OH)□·8H□O	Fisher Scientific
	Carbonate: 1.9–4.7 mM Na□CO□	
Halides	Bromide: 0.6mM of NaBr	Sigma Aldrich
	Iodide: 400nM of NaI	Fisher Scientific
pH	6 – 8	HCl: J.T. Baker
	Adjusted using HCl and NaOH	NaOH: Fisher Scientific

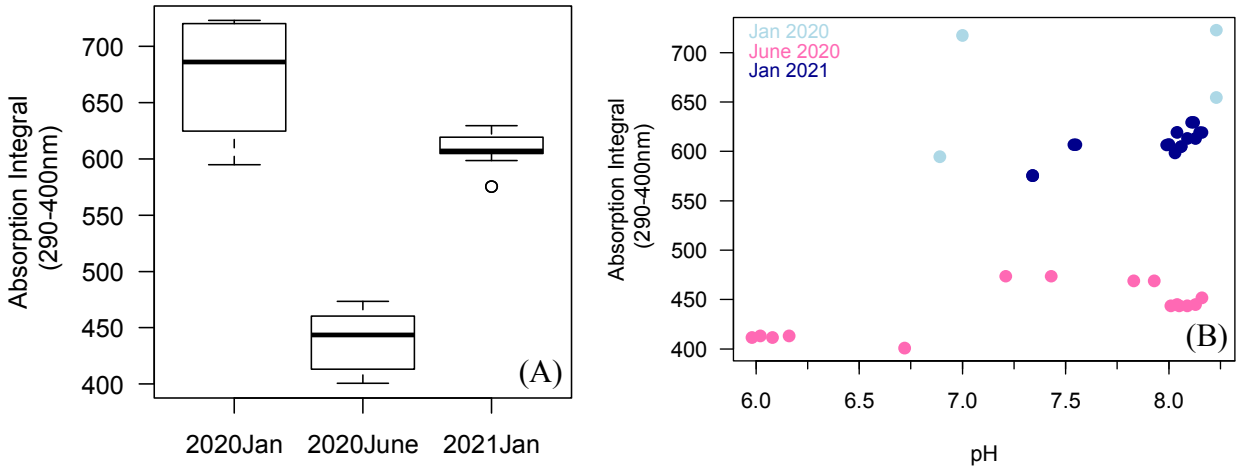

Figure 1. Seasonal variability and pH effects on CDOM absorption over 290–400 nm. A) Mean absorption integrals were statistically different for between three dates of collection (df=2, F=201, $p<10^{-16}$). B) Absorption integral and pH had a positive correlation within each collection groups. However, correlations were greater for June 2020 (r=0.72, p=0.638) and January 2021 (r=0.79, p=0.003) groups than the January 2020 group (r=0.36, p<0.001).

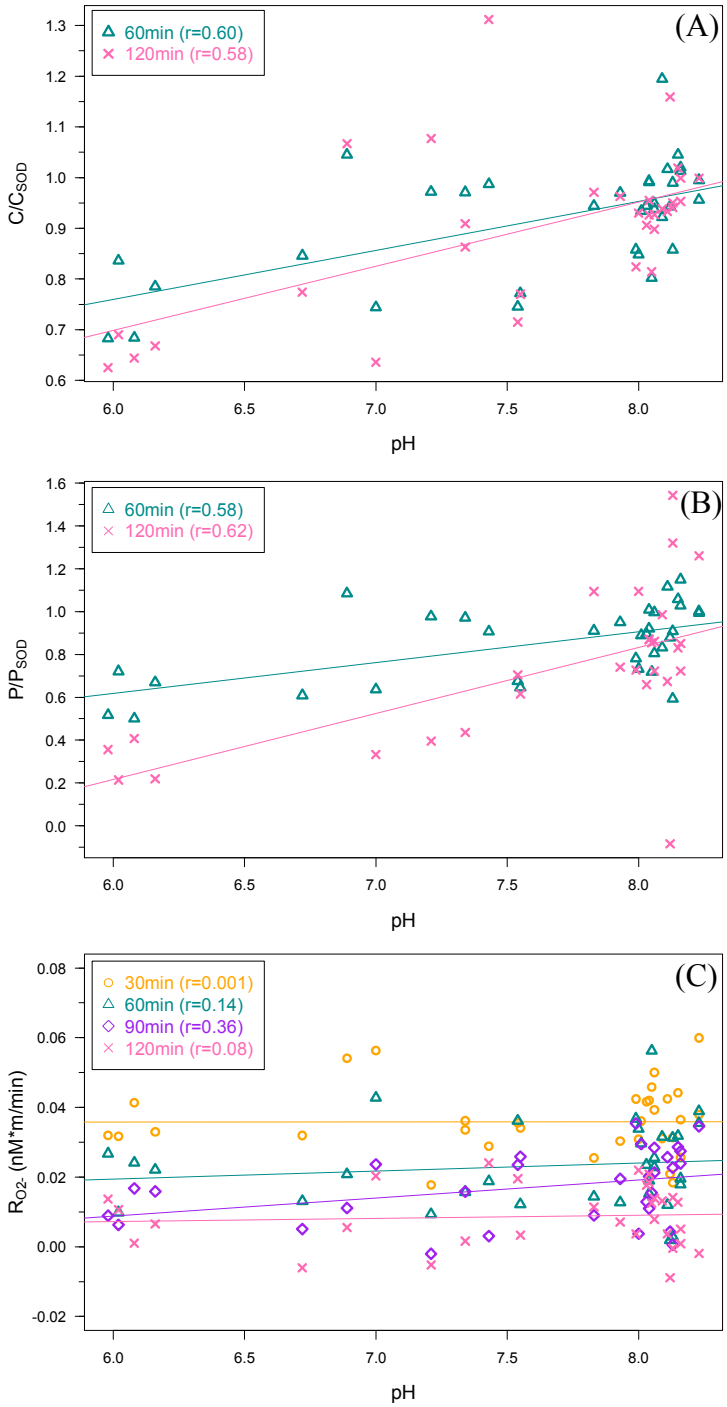

Figure 2. The effect of pH on superoxide decay pathways and maximal photoproduction rates. A) C/C_{SOD} is significantly correlated to pH (60: r=0.60, p=0.0002; 120: r=0.58, p=0.0005). B) P/P_{SOD} is significantly correlated to pH (60: r=0.58, p=0.0004; 120: r=0.62, p=0.0004). C) R_{O2-} is not significantly correlated to pH, except 60–90min (r=0.36, p=0.045).

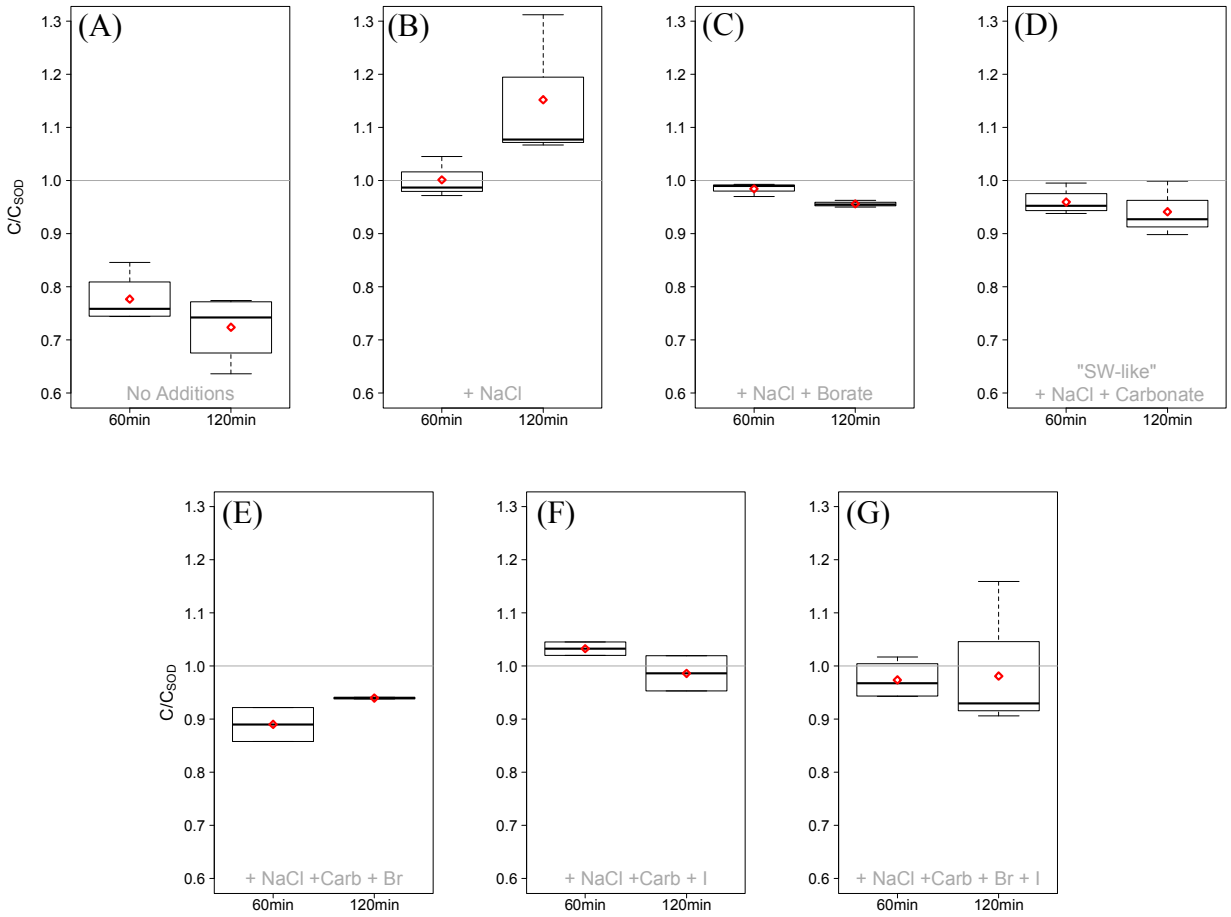

Figure 3. Effect of various chemical additions on C/C$_{SOD}$ during 2-hrs of irradiation in freshwater solutions. Red diamond represents the mean C/C$_{SOD}$. See Table 2a for time statistical break down; see Table S2a for chemical addition breakdown.

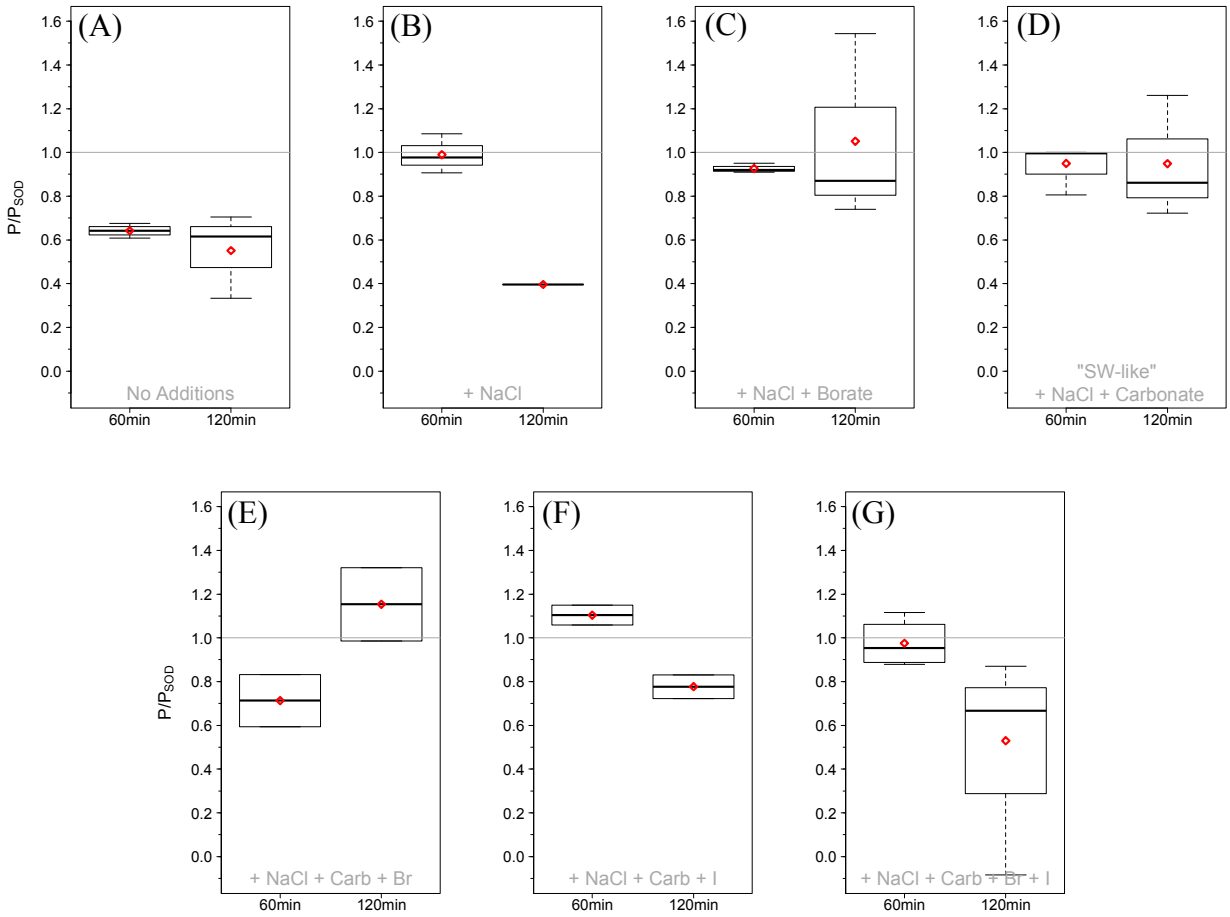

Figure 4. Effect of various chemical additions on P/P$_{SOD}$ during 2-hrs of irradiation in freshwater solutions. Red diamond represents the mean P/P$_{SOD}$. See Table 2b for time statistical break down; see Table S2b for chemical addition breakdown.

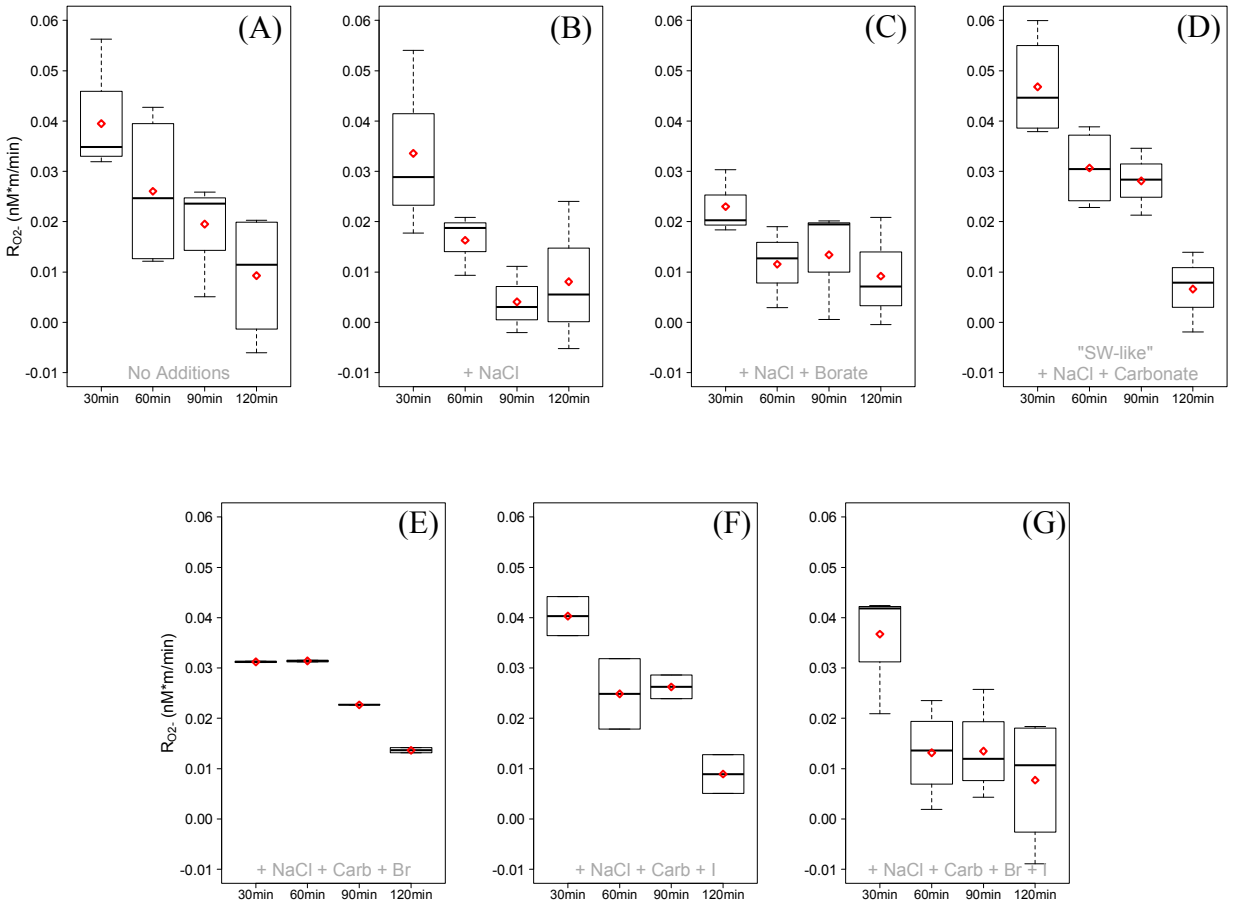

Figure 5. Effect of various chemical additions on R_{O2-} during 2-hrs of irradiation in freshwater solutions. Red diamond represents the mean R_{O2-}. See Table 1c for time statistical break down; see Table S2c for chemical addition breakdown.

Table 2. Mean superoxide decay ratios and photoproduction rates of chemical additions during 2-hrs of irradiation.

(A) Concentration Ratio, C/C_{SOD}						
t-test	**60 min**	**120 min**	**Mean difference**	**t**	**df**	**p-value**
No Additions	0.777 ± 0.048	0.724 ± 0.064	-0.053	1.3	5.5	0.239
+ NaCl	1.001 ± 0.039	1.152 ± 0.139	0.151	1.8	2.3	0.194
+ NaCl + Borate	0.984 ± 0.013	0.956 ± 0.007	-0.028	3.5	3.0	0.040*
+ NaCl + Carbonate	0.960 ± 0.025	0.941 ± 0.052	-0.018	0.6	2.7	0.619
+ NaCl + Carb + Bromide	0.890 ± 0.045	0.940 ± 0.002	0.050	1.5	1.0	0.365
+ NaCl + Carb + Iodide	1.033 ± 0.018	0.986 ± 0.047	-0.047	1.3	1.3	0.375
+ NaCl + Carb + Br + I	0.974 ± 0.037	0.981 ± 0.119	0.007	0.1	3.6	0.914

(B) Rate Ratio, P/P_{SOD}						
t-test	**0–60 min**	**60–120 min**	**Mean difference**	**t**	**df**	**p-value**
No Additions	0.642 ± 0.027	0.551 ± 0.194	-0.090	0.8	2.1	0.505
+ NaCl	0.990 ± 0.090	0.396‡	-0.594	—	—	—
+ NaCl + Borate	0.927 ± 0.022	1.051 ± 0.431	0.124	0.5	2.0	0.667
+ NaCl + Carbonate	0.950 ± 0.096	0.948 ± 0.279	-0.001	0.0	2.4	0.995
+ NaCl + Carb + Bromide	0.713 ± 0.168	1.154 ± 0.237	0.441	2.1	1.8	0.179
+ NaCl + Carb + Iodide	1.104 ± 0.065	0.777 ± 0.076	-0.327	4.6	2.0	0.046*
+ NaCl + Carb + Br + I	0.975 ± 0.110	0.530 ± 0.420	-0.446	2.1	3.4	0.122

(C) Max Superoxide Rate, R_{O2-}								
Pearson's Correlation	**0–30 min**	**30–60 min**	**60–90 min**	**90–120 min**	**cor**	**t**	**df**	**p-value**
No Additions	0.0395 ± 0.011	0.0260 ± 0.016	0.0195 ± 0.0097	0.00928 ± 0.013	-0.70	3.7	14	0.002*
+ NaCl	0.0336 ± 0.019	0.0163 ± 0.006	0.0040 ± 0.0066	0.00809 ± 0.015	-0.65	2.7	10	0.023*
+ NaCl + Borate	0.0230 ± 0.006	0.0115 ± 0.008	0.0134 ± 0.0111	0.00917 ± 0.011	-0.48	1.7	10	0.115
+ NaCl + Carbonate	0.0468 ± 0.010	0.0307 ± 0.008	0.0281 ± 0.0066	0.00661 ± 0.008	-0.86	5.9	12	0.0001*
+ NaCl + Carb + Br	0.0312 ± 0.000	0.0314 ± 0.000	0.0227‡	0.01365 ± 0.001	-0.94	-6.2	5	0.002*
+ NaCl + Carb + I	0.0403 ± 0.005	0.0249 ± 0.010	0.0262 ± 0.0033	0.00892 ± 0.005	-0.86	4.2	6	0.006*
+ NaCl + Carb + Br + I	0.0367± 0.011	0.0132 ± 0.009	0.0135 ± 0.0090	0.00772 ± 0.013	-0.67	3.4	14	0.004*

‡ Not enough data available for standard deviations

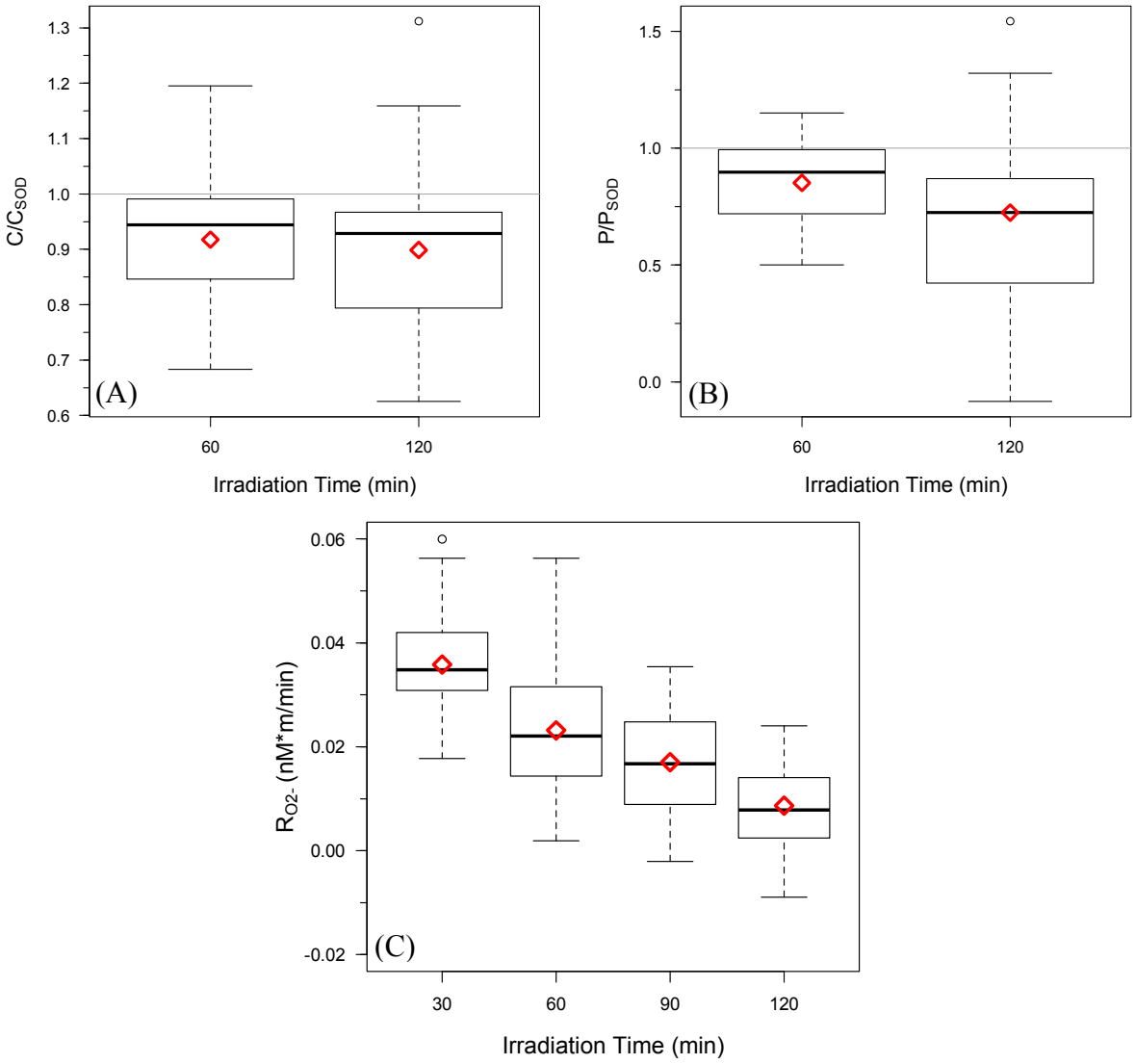

Figure 6. Superoxide decay pathways and maximal superoxide photoproduction rates of all samples over 2-hrs of irradiation. Red diamond represents the mean. A) C/C_{SOD} does not significantly change with time across all samples (p=0.576). B) P/ P_{SOD} does not significantly change with time across all samples, though there seems to be a small decrease in the second hour of irradiation (p=0.099). C) R_{O2-} is significantly correlated to irradiation time (r=–0.69, $p<10^{-16}$)

Acknowledgments

This work was supported by NSF grant OCE-1924763. We would like to thank Leanne Powers and Amanda Frossard for their contributions to this work.

References

Barkley, R. A., & Thompson, T. G. (1960). The total iodine and iodate-iodine content of sea-water. *Deep Sea Research (1953), 7*(1), 24-34. doi: 10.1016/0146-6313(60)90004-6

Bielski, B. H., Cabelli, D. E., Arudi, R. L., & Ross, A. B. (1985). Reactivity of HO2/O− 2 radicals in aqueous solution. *Journal of physical and chemical reference data, 14*(4), 1041-1100. doi: 10.1063/1.555739

Blough, N. (1997). Photochemistry in the sea-surface microlayer. In P. S. Liss & R. A. Duce (Eds.), *The Sea Surface and Global Change* (pp. 383-424): Cambridge University Press.

Blough, N. V., & Zepp, R. G. (1995). Reactive oxygen species in natural waters. In *Active oxygen in chemistry* (pp. 280-333): Springer. doi:10.1007/978-94-007-0874-7_8

Burns, J. M., Cooper, W. J., Ferry, J. L., King, D. W., DiMento, B. P., McNeill, K., Miller, C. J., Miller, W. L., Peake, B. M., Rusak, S. A., Rose, A. L., & Waite, T. D. (2012). Methods for reactive oxygen species (ROS) detection in aqueous environments. *Aquatic Sciences, 74*(4), 683-734. doi: 10.1007/s00027-012-0251-x

Clark, C. D., & Zika, R. G. (2000). Marine organic photochemistry: from the sea surface to marine aerosols. In *Marine Chemistry* (pp. 1-33): Springer. doi:10.1007/10683826_1

Coble, P. G. (2008). Marine Optical Biogeochemistry: The Chemistry of Ocean Color. *Chemical reviews, 107*(2), 402-418. doi: 10.1021/cr050350

Dong, Y., Peng, W., Liu, Y., & Wang, Z. (2021). Photochemical origin of reactive radicals and halogenated organic substances in natural waters: A review. *Journal of Hazardous Materials, 401*, 123884. doi: 10.1016/j.jhazmat.2020.123884

Fujii, M., & Otani, E. (2017). Photochemical generation and decay kinetics of superoxide and hydrogen peroxide in the presence of standard humic and fulvic acids. *Water Research, 123*, 642-654. doi: 10.1016/j.watres.2017.07.015

Gao, H., & Zepp, R. G. (1998). Factors influencing photoreactions of dissolved organic matter in a coastal river of the southeastern United States. *Environmental science & technology, 32*(19), 2940-2946. doi: 10.1021/es9803660

Garg, S., Rose, A. L., & Waite, T. D. (2011). Photochemical production of superoxide and hydrogen peroxide from natural organic matter. *Geochimica et Cosmochimica Acta, 75*(15), 4310-4320. doi: 10.1016/j.gca.2011.05.014

Glover, C. M., & Rosario-Ortiz, F. L. (2013). Impact of halides on the photoproduction of reactive intermediates from organic matter. *Environmental science & technology, 47*(24), 13949-13956. doi: 10.1021/es4026886

Goldstone, J. V., & Voelker, B. M. (2000). Chemistry of superoxide radical in seawater: CDOM associated sink of superoxide in coastal waters. *Environmental science & technology, 34*(6), 1043-1048. doi: 10.1021/es9905445

Grebel, J. E., Pignatello, J. J., Song, W., Cooper, W. J., & Mitch, W. A. (2009). Impact of halides on the photobleaching of dissolved organic matter. *Marine Chemistry, 115*(1-2), 134-144. doi: 10.1016/j.marchem.2009.07.009

Hansel, C. M., & Diaz, J. M. (2021). Production of extracellular reactive oxygen species by marine biota. *Annual review of marine science, 13*, 177-200. doi: 10.1146/annurev-marine-041320-102550

Heller, M., & Croot, P. (2010a). Kinetics of superoxide reactions with dissolved organic matter in tropical Atlantic surface waters near Cape Verde (TENATSO). *Journal of Geophysical Research: Oceans, 115*(C12). doi: 10.1029/2009JC006021

Heller, M. I., & Croot, P. L. (2010b). Superoxide decay kinetics in the Southern Ocean. *Environmental science & technology, 44*(1), 191-196. doi: 10.1021/es901766r

Heller, M. I., Wuttig, K., & Croot, P. L. (2016). Identifying the sources and sinks of CDOM/FDOM across the Mauritanian Shelf and their potential role in the decomposition of superoxide (O2-). *Frontiers in Marine Science, 3*, 132. doi: 10.3389/fmars.2016.00132

Ho, R. Y., Liebman, J. F., & Valentine, J. S. (1995). Overview of the Energetics and Reactivity of Oxygen. In *Active Oxygen in Chemistry* (pp. 1-23): Springer. doi: 10.1007/978-94-007-0874-7_1

Jammoul, A., Dumas, S., D'anna, B., & George, C. (2009). Photoinduced oxidation of sea salt halides by aromatic ketones: a source of halogenated radicals. *Atmospheric Chemistry and Physics, 9*(13), 4229-4237. doi: 10.5194/acp-9-4229-2009

Jiao, X., Zeng, R., Lan, G., Zuo, S., He, J., & Wang, C. (2022). Mechanistic study on photochemical generation of I•/I2•− radicals in coastal atmospheric aqueous aerosol. *Science of The Total Environment*, 154080. doi: 10.1016/j.scitotenv.2022.154080

Kieber, D. J., Peake, B. M., & Scully, N. M. (2003). Reactive oxygen species in aquatic ecosystems. In E. W. Helbling & H. Zagarese (Eds.), *UV Effects in Aquatic Organisms and Ecosystems* (Vol. 1, pp. 251-288): The Royal Society of Chemistry. doi: 10.1039/9781847552266-00251

King, D. W., Cooper, W. J., Rusak, S. A., Peake, B. M., Kiddle, J. J., O'Sullivan, D. W., Melamed, M. L., Morgan, C. R., & Theberge, S. M. (2007). Flow injection analysis of H2O2 in natural waters using acridinium ester chemiluminescence: method development and optimization using a kinetic model. *Analytical chemistry, 79*(11), 4169-4176. doi: 10.1021/ac062228w

King, D. W., Berger, E., Helm, Z., Irish, E., & Mopper, K. (2016). Measurement of antioxidant activity toward superoxide in natural waters. *Frontiers in Marine Science, 3*, 217. doi: 10.3389/fmars.2016.00217

Koch, B. P., Witt, M., Engbrodt, R., Dittmar, T., & Kattner, G. (2005). Molecular formulae of marine and terrigenous dissolved organic matter detected by electrospray ionization Fourier transform ion cyclotron resonance mass spectrometry. *Geochimica et Cosmochimica Acta, 69*(13), 3299-3308. doi: 10.1016/j.gca.2005.02.027

Le Roux, D. M., Powers, L. C., & Blough, N. V. (2021). Photoproduction rates of one-electron reductants by chromophoric dissolved organic matter via fluorescence spectroscopy: comparison with superoxide and hydrogen peroxide rates. *Environmental science & technology, 55*(17), 12095-12105. doi: 10.1021/acs.est.1c04043

Lu, Q., Yuan, Y., Tao, Y., & Tang, J. (2015). Environmental pH and ionic strength influence the electron-transfer capacity of dissolved organic matter. *Journal of Soils and Sediments, 15*(11), 2257-2264. doi: 10.1007/s11368-015-1154-y

Ma, J., Nie, J., Zhou, H., Wang, H., Lian, L., Yan, S., & Song, W. (2020). Kinetic Consideration of Photochemical Formation and Decay of Superoxide Radical in Dissolved Organic Matter Solutions. *Environmental science & technology, 54*(6), 3199-3208. doi: 10.1021/acs.est.9b06018

Méndez-Díaz, J. D., Shimabuku, K. K., Ma, J., Enumah, Z. O., Pignatello, J. J., Mitch, W. A., & Dodd, M. C. (2014). Sunlight-driven photochemical halogenation of dissolved organic matter in seawater: A natural abiotic source of organobromine and organoiodine. *Environmental science & technology, 48*(13), 7418-7427. doi: 10.1021/es5016668

Meyers-Schulte, K. J., & Hedges, J. I. (1986). Molecular evidence for a terrestrial component of organic matter dissolved in ocean water. *Nature, 321*(6065), 61-63. doi: 10.1038/321061a0

Micinski, E., Ball, L. A., & Zafiriou, O. C. (1993). Photochemical oxygen activation: Superoxide radical detection and production rates in the eastern Caribbean. *Journal of Geophysical Research: Oceans, 98*(C2), 2299-2306. doi: 10.1029/92JC02766

Miller, W. L., & Kester, D. R. (1988). Hydrogen peroxide measurement in seawater by (p-hydroxyphenyl) acetic acid dimerization. *Analytical chemistry, 60*(24), 2711-2715. doi: 10.1021/ac00175a014

Moffett, J. W., & Zafiriou, O. C. (1993). The photochemical decomposition of hydrogen peroxide in surface waters of the eastern Caribbean and Orinoco River. *Journal of Geophysical Research: Oceans, 98*(C2), 2307-2313. doi: 10.1029/92JC02768

Moore, R. J. (1999). *Photochemical degradation of coloured dissolved organic matter in two Nova Scotia Lakes.* (M.Sc.). Dalhousie University, Halifax, NS.

Moore, R. M., & Zafiriou, O. C. (1994). Photochemical production of methyl iodide in seawater. *Journal of Geophysical Research: Atmospheres, 99*(D8), 16415-16420. doi: 10.1029/94JD00786

Mopper, K., & Zhou, X. (1990). Hydroxyl radical photoproduction in the sea and its potential impact on marine processes. *Science, 250*(4981), 661-664. doi: 10.1126/science.250.4981.661

Opsahl, S., & Benner, R. (1997). Distribution and cycling of terrigenous dissolved organic matter in the ocean. *Nature, 386*(6624), 480-482. doi: 10.1038/386480a0

Pace, M. L., Reche, I., Cole, J. J., Fernández-Barbero, A., Mazuecos, I. P., & Prairie, Y. T. (2012). pH change induces shifts in the size and light absorption of dissolved organic matter. *Biogeochemistry, 108*(1), 109-118. doi: 10.1007/s10533-011-9576-0

Parker, K. M., & Mitch, W. A. (2016). Halogen radicals contribute to photooxidation in coastal and estuarine waters. *Proceedings of the National Academy of Sciences, 113*(21), 5868-5873. doi: 10.1073/pnas.1602595113

Petasne, R. G., & Zika, R. G. (1987). Fate of superoxide in coastal sea water. *Nature, 325*(6104), 516-518. doi: 10.1038/325516a0

Powers, L. C., & Miller, W. L. (2014). Blending remote sensing data products to estimate photochemical production of hydrogen peroxide and superoxide in the surface ocean. *Environmental Science: Processes & Impacts, 16*(4), 792-806. doi: 10.1039/C3EM00617D

Powers, L. C., Babcock-Adams, L. C., Enright, J. K., & Miller, W. L. (2015). Probing the photochemical reactivity of deep ocean refractory carbon (DORC): lessons from hydrogen peroxide and superoxide kinetics. *Marine Chemistry, 177*, 306-317. doi: 10.1016/j.marchem.2015.06.005

Powers, L. C., & Miller, W. L. (2016). Apparent quantum efficiency spectra for superoxide photoproduction and its formation of hydrogen peroxide in natural waters. *Frontiers in Marine Science, 3*, 235. doi: 10.3389/fmars.2016.00235

R Core Team (2020). R: A Language and Environment for Statistical Computing. R Foundation for Statistical Computing. Vienna, Austria. Retrieved from https://www.R-project.org/

Shaked, Y., Harris, R., & Klein-Kedem, N. (2010). Hydrogen peroxide photocycling in the Gulf of Aqaba, Red Sea. *Environmental science & technology, 44*(9), 3238-3244. doi: 10.1021/es902343y

Sharpless, C. M., & Blough, N. V. (2014). The importance of charge-transfer interactions in determining chromophoric dissolved organic matter (CDOM) optical and photochemical properties. *Environmental Science: Processes & Impacts, 16*(4), 654-671. doi: 10.1039/C3EM00573A

Sleighter, R. L., & Hatcher, P. G. (2008). Molecular characterization of dissolved organic matter (DOM) along a river to ocean transect of the lower Chesapeake Bay by ultrahigh resolution electrospray ionization Fourier transform ion cyclotron resonance mass spectrometry. *Marine Chemistry, 110*(3-4), 140-152. doi: 10.1016/j.marchem.2008.04.008

Spencer, R. G., Bolton, L., & Baker, A. (2007). Freeze/thaw and pH effects on freshwater dissolved organic matter fluorescence and absorbance properties from a number of UK locations. *Water Research, 41*(13), 2941-2950. doi: 10.1016/j.watres.2007.04.012.

Sutherland, K. M., Wankel, S. D., & Hansel, C. M. (2020). Dark biological superoxide production as a significant flux and sink of marine dissolved oxygen. *Proceedings of the National Academy of Sciences, 117*(7), 3433-3439. doi: 10.1073/pnas.1912313117

Tang, X., Cui, Z., Bai, Y., & Su, R. (2021). Indirect photodegradation of sulfathiazole and sulfamerazine: Influence of the CDOM components and seawater factors (salinity, pH, nitrate and bicarbonate). *Science of The Total Environment, 750*, 141762. doi: 10.1016/j.scitotenv.2020.141762

Twardowski, M. S., Boss, E., Sullivan, J. M., & Donaghay, P. L. (2004). Modeling the spectral shape of absorption by chromophoric dissolved organic matter. *Marine Chemistry, 89*(1-4), 69-88. doi: 10.1016/j.marchem.2004.02.008

Vione, D., Minella, M., Maurino, V., & Minero, C. (2014). Indirect photochemistry in sunlit surface waters: photoinduced production of reactive transient species. *Chemistry–A European Journal, 20*(34), 10590-10606. doi: 10.1002/chem.201400413

Voelker, B. M., Sedlak, D. L., & Zafiriou, O. C. (2000). Chemistry of superoxide radical in seawater: Reactions with organic Cu complexes. *Environmental science & technology, 34*(6), 1036-1042. doi: 10.1021/es990545x

Wuttig, K., Heller, M. I., & Croot, P. L. (2013). Pathways of superoxide (O2–) decay in the Eastern Tropical North Atlantic. *Environmental science & technology, 47*(18), 10249-10256. doi: 10.1021/es401658t

Yan, S., Liu, Y., Lian, L., Li, R., Ma, J., Zhou, H., & Song, W. (2019). Photochemical formation of carbonate radical and its reaction with dissolved organic matters. *Water Research, 161*, 288-296. doi: 10.1016/j.watres.2019.06.002

Yang, Y., & Pignatello, J. J. (2017). Participation of the halogens in photochemical reactions in natural and treated waters. *Molecules, 22*(10), 1684. doi: 10.3390/molecules22101684

Zafiriou, O. C., Joussot-Dubien, J., Zepp, R. G., & Zika, R. G. (1984). Photochemistry of natural waters. *Environmental science & technology, 18*(12), 358A-371A.

Zepp, R. G., & Schlotzhauer, P. F. (1981). Comparison of photochemical behavior of various humic substances in water: III. Spectroscopic properties of humic substances. *Chemosphere, 10*(5), 479-486. doi: 10.1016/0045-6535(81)90148-X

Zhang, Y., Del Vecchio, R., & Blough, N. V. (2012). Investigating the mechanism of hydrogen peroxide photoproduction by humic substances. *Environmental science & technology, 46*(21), 11836-11843. doi: 10.1021/es3029582

Zhang, Y., & Blough, N. V. (2016). Photoproduction of one-electron reducing intermediates by chromophoric dissolved organic matter (CDOM): relation to O2–and H2O2 photoproduction and CDOM photooxidation. *Environmental science & technology, 50*(20), 11008-11015. doi: 10.1021/acs.est.6b02919

Zhang, Y., Zhou, L., Zhou, Y., Zhang, L., Yao, X., Shi, K., Jeppesen, E., Yu, Q., & Zhu, W. (2021). Chromophoric dissolved organic matter in inland waters: Present knowledge and future challenges. *Science of The Total Environment, 759*, 143550. doi: 10.1016/j.scitotenv.2020.143550

Zhang, Y. N., Zhao, J., Zhou, Y., Qu, J., Chen, J., Li, C., Qin, W., Zhao, Y., & Willie, J. G. (2019). Combined effects of dissolved organic matter, pH, ionic strength and halides on photodegradation of oxytetracycline in simulated estuarine waters. *Environmental Science: Processes & Impacts, 21*(1), 155-162. doi: 10.1039/c8em00473k

CHAPTER 3

CONCLUSIONS AND FUTURE DIRECTIONS

The processes that control redox reactions, the fate of oxygen, and superoxide cycling in natural waters, especially during solar irradiation, are not completely understood. Data gaps in O_2^- photoproduction rates, decay kinetics, and apparent quantum yield (AQY) spectra make it difficult to quantify the photo-efficiency for O_2^- production. Elucidating superoxide's photochemical and subsequent thermal pathways is essential to understanding the marine oxygen budget across aquatic ecosystems and diel cycles (Sutherland et al., 2020). Should superoxide reduction pathways dominate, major O_2 loss in the marine oxygen cycle could occur. Therefore, this thesis aims to identify and potentially quantify the environmental and chemical parameters that control superoxide pathways as a contribution to ultimately improving the accuracy of photoproduction estimates and photochemical cycling models.

Previous studies using the enzyme SOD as a quantitative trap for photochemical production of O_2^- have concluded by comparison to untreated samples that dismutation to H_2O_2 may not always be the primary sink for O_2^-, as once assumed, and that oxidative pathways make up between 40–70% of O_2^- reactions in seawater (Petasne & Zika, 1987; Garg et al., 2011; Powers & Miller, 2016). Therefore, a 2:1 assumption used to back-calculate R_{O2-} from environmental H_2O_2 photoproduction rates could grossly underestimate the predicted photochemical rates of superoxide. This observation, additionally, aligns with recent work using one-electron reductants that observed a significant oxidative sink for O_2^- around 65–88% and

suggest that this could result from the simultaneous photoproduction of phenoxy radicals with CDOM (Zhang & Blough, 2016; Le Roux et al., 2021).

The work presented in this thesis addresses these O_2^- sinks in the sun by using SOD to elucidate the relative O_2^- oxidative or reductive decay pathways among environmental and chemical parameters relevant to seawater, including CDOM, pH, ionic strength, carbonate interactions, and halide effects. The results in Chapter 2 indicate that oxidative pathways, as represented by C/C_{SOD} and P/P_{SOD}, decrease with increased pH and NaCl additions. Halide additions, however, provide largely inconclusive results, though Br^- and I^- seem to slightly decrease and increase, respectively, both C/C_{SOD} and P/P_{SOD} during the first hour of irradiation. In contrast, the most notable chemical control on R_{O2-} was carbonate buffer, suggesting that carbonate radical may play an additional complex role in the photochemical cycling of ROS in surface seawater.

The most striking trend across all our data was the significant decline in R_{O2-} during 2 hours of irradiation. We speculate this the nonlinear accumulation of H_2O_2 over irradiation is most likely due to decreased electron availability to oxygen as a result of competition with photochemically produced one-electron reductants within CDOM ($CDOM^{+/-}$). While not statistically significant, we also observed a slight enhancement in oxidative pathways with continued irradiation as represented by C/C_{SOD} and P/P_{SOD}. We suggest that this increase in oxidative pathways in the light may be due to the simultaneous photoproduction of $CDOM^+$ during the initial electron-transfer to O_2, ultimately building a pool of oxidants that may, in turn start to compete with O_2 for electrons made available with photochemistry. Additionally, we suggest our calculated R_{O2-} may underestimate superoxide production rates by as much as 10% due to H_2O_2 photodecomposition. Altogether, the results presented in this study imply there are

shifts in O_2^- decay pathways and production rates that seem to fluctuate across natural water environments and with diel cycles.

Future work would benefit from examining marine DOM photoreactivity and superoxide cycling in natural systems. The molecular differences between freshwater and seawater DOM could influence CDOM photochemical efficiency. Additional studies that use DOM isolated from known marine sources, added to Milli-Q water and "built" back toward seawater conditions as was done here with a freshwater DOM may reveal ROS redox pathways and photoreactivity differences between marine and freshwater DOM. Thus, further research of the environmental and chemical controls on superoxide pathways examined in this study is needed before results from this study can be extrapolated to better predict rates of superoxide production and decay in open ocean systems.

Further investigations into the role of photo-oxidants on O_2^- production and decay would also enrich our understanding of redox potential and the fate of O_2 in natural sunlit waters. To date, superoxide decay rates have been determined post-irradiation, and therefore, may not account for an additional loss by a photochemical produced transient species (Powers & Miller, 2016). The results of this study would be further supported by quantifying O_2^- reactivity using "antioxidant" activity analysis (King et al., 2016) during dark and irradiated experiments with these same environmental and chemical parameters. Additionally, investigations into the overall redox state of surface sweater in the dark and light may reveal links to a photo-oxidized DOM pool. Altogether, these and future studies will illuminate the parameters that control O_2^- reaction pathways in irradiated samples and identify additional studies that are needed to model ROS kinetics. Ultimately, we hope work done in this thesis leads to a deeper understanding of the role of photochemistry in biogeochemical cycling and the redox state of sunlit natural waters.

References

Garg, S., Rose, A. L., & Waite, T. D. (2011). Photochemical production of superoxide and hydrogen peroxide from natural organic matter. *Geochimica et Cosmochimica Acta, 75*(15), 4310-4320. doi: 10.1016/j.gca.2011.05.014

King, D. W., Berger, E., Helm, Z., Irish, E., & Mopper, K. (2016). Measurement of antioxidant activity toward superoxide in natural waters. *Frontiers in Marine Science, 3*, 217. doi: 10.3389/fmars.2016.00217

Le Roux, D. M., Powers, L. C., & Blough, N. V. (2021). Photoproduction rates of one-electron reductants by chromophoric dissolved organic matter via fluorescence spectroscopy: comparison with superoxide and hydrogen peroxide rates. *Environmental science & technology, 55*(17), 12095-12105. doi: 10.1021/acs.est.1c04043

Petasne, R. G., & Zika, R. G. (1987). Fate of superoxide in coastal sea water. *Nature, 325*(6104), 516-518. doi: 10.1038/325516a0

Powers, L. C., & Miller, W. L. (2016). Apparent quantum efficiency spectra for superoxide photoproduction and its formation of hydrogen peroxide in natural waters. *Frontiers in Marine Science, 3*, 235. doi: 10.3389/fmars.2016.00235

Sutherland, K. M., Wankel, S. D., & Hansel, C. M. (2020). Dark biological superoxide production as a significant flux and sink of marine dissolved oxygen. *Proceedings of the National Academy of Sciences, 117*(7), 3433-3439. doi: 10.1073/pnas.1912313117

Zhang, Y., & Blough, N. V. (2016). Photoproduction of one-electron reducing intermediates by chromophoric dissolved organic matter (CDOM): relation to O2–and H2O2 photoproduction and CDOM photooxidation. *Environmental science & technology, 50*(20), 11008-11015. doi: 10.1021/acs.est.6b02919

APPENDICES

SUPPORTING INFORMATION

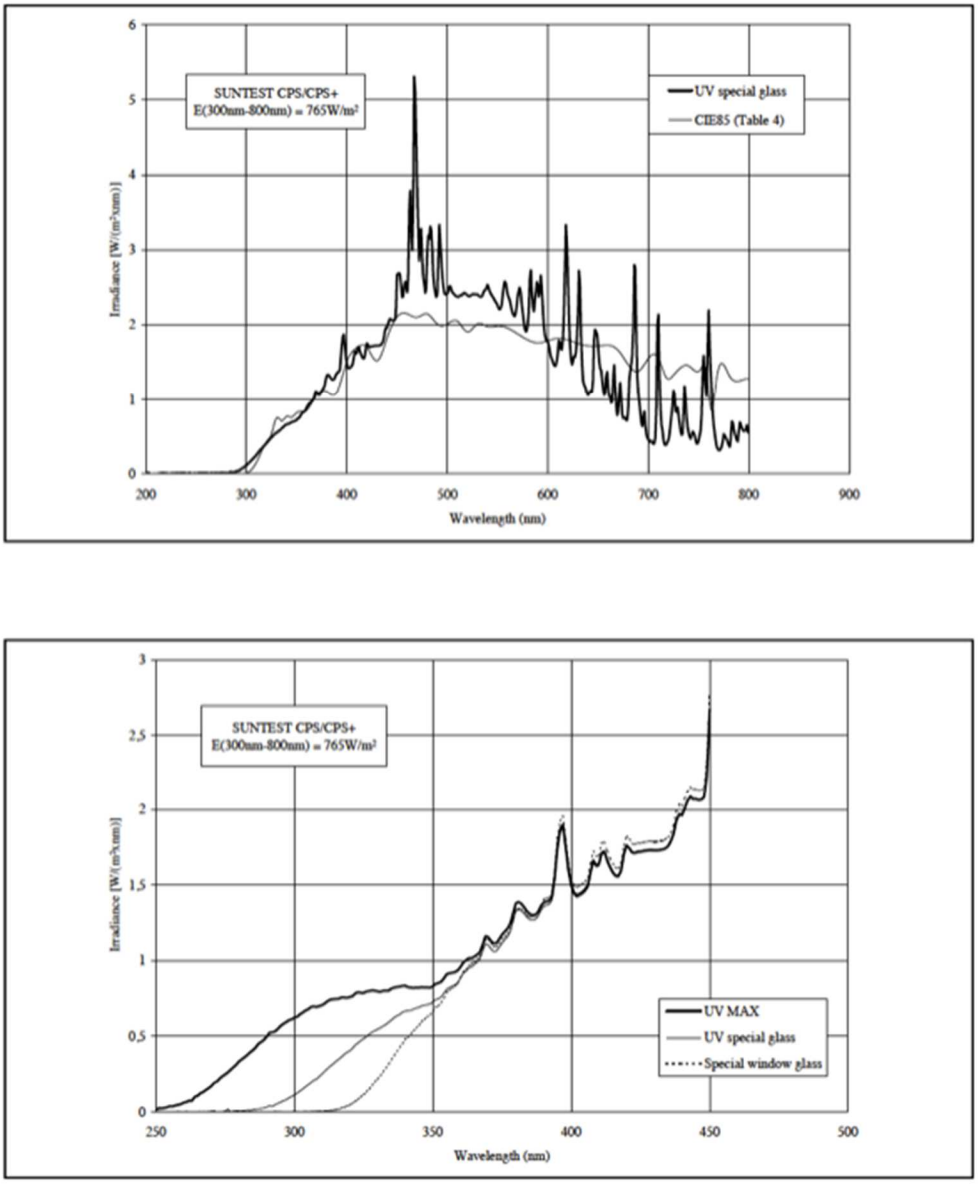

Figure S1. Suntest CPS special window glass. Solar simulator equipped with a 1.5 kW xenon lamp (Atlas) fitted with IR-filtering window glass that simulates sunlight reaching the earth's surface (290–800 nm) was used for irradiation experiments. From Suntest CPS Manufacturer.

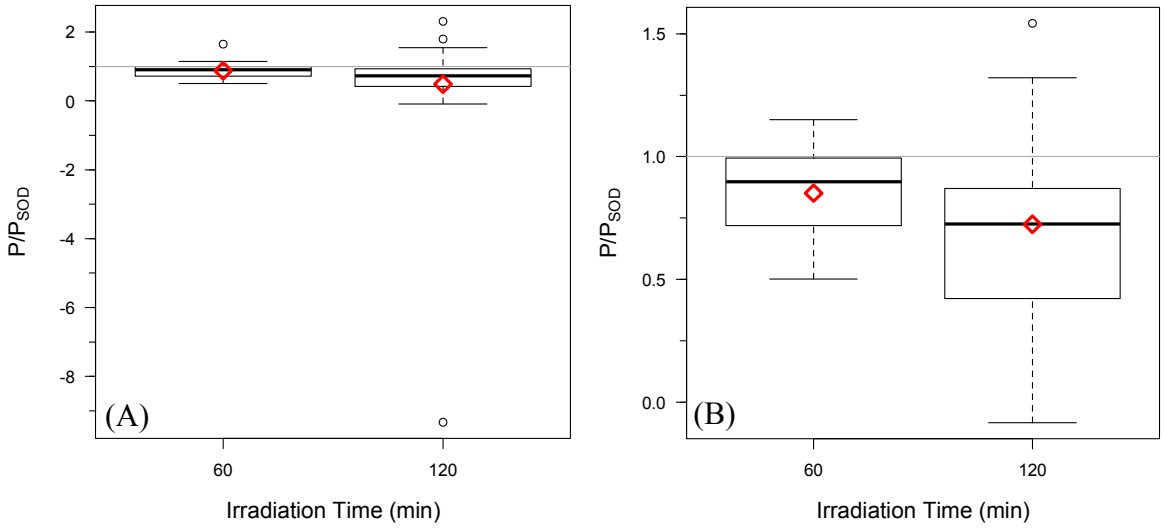

Figure S2. P/P$_{SOD}$ across all samples was largely variable with distinct outliers. A) Unamended data gave drastic outliers, therefore outliers (4) were removed to better understand our data. B) Even with outliers removed, the rate ratio for all samples did not statistically change over time, though the mean difference is slightly lower for final rate ratios (t=1.7, df=38, p=0.099).

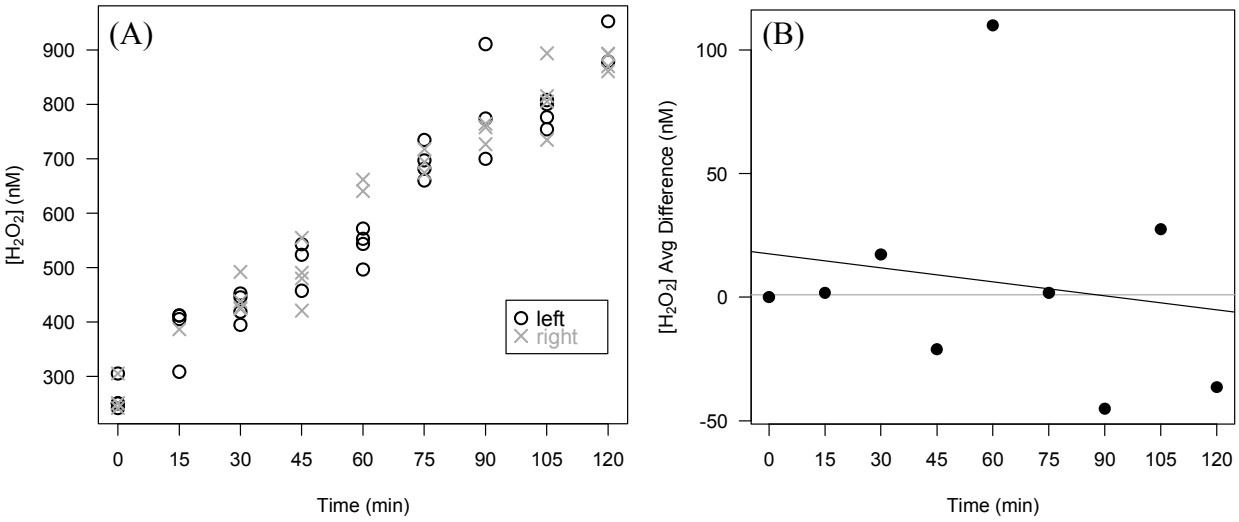

Figure S3. H_2O_2 photoproduction relative to position under solar simulator. A one sample t-test was performed in R to compare the mean differences of H_2O_2 concentration between the positions of beakers. The average difference in mean $[H_2O_2]$ for all time points was 6.2 ± 45 nM and is not statistically significant (t=0.41, df=8, p=0.69).

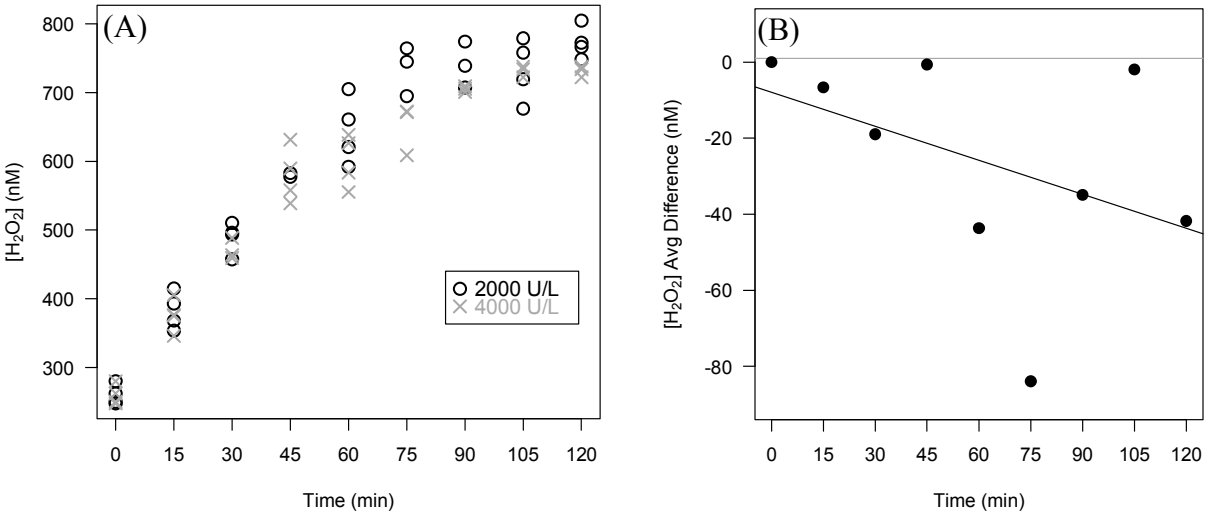

Figure S4. H_2O_2 photoproduction in freshwater solutions containing 2000 U/L or 4000 U/L of SOD. A) Two freshwater solutions with 2000U/L and 4000U/L SOD, respectively, were irradiated for 2-hrs to determine maximal SOD activity. B) The average difference of $[H_2O_2]$ was calculated for each 15-min sampling to determine the overall average mean difference. A one sample t-test performed in R on these mean differences showed 4000U/L SOD to have a small decrease from 2000U/L (t=2.6, df=8, p=0.025) within analytical uncertainty.

Table S1. Percent absorption fading across all samples from 290–400 nm

ID	Collection	pH	Chemical Additions	% Fading $a_{(290–400)}$
A1-1	Jan2020	7.00	None	-9.2%
A2-1	Jan2020	8.23	+Carb+NaCl	-1.3%
A3-1	Jan2020	6.89	+NaCl	+2.7%
A2-2	Jan2020	8.23	+Carb+NaCl	-1.5%
B1-1	June2020	6.72	None	+17.8%
B2-1	June2020	8.01	+Bor	-4.5%
B2-2	June2020	8.05	+Bor	-4.4%
B2-3	June2020	8.09	+Bor	-3.6%
B3-1	June2020	8.13	+Bor+NaCl	-4.0%
B3-2	June2020	8.04	+Bor+NaCl	-6.0%
B4-1	June2020	7.21	+NaCl	-17.4%
B4-2	June2020	7.43	+NaCl	-13.3%
B5-1	June2020	6.08	None	-2.8%
B5-2	June2020	5.98	None	-3.4%
B6-1	June2020	6.02	+Bor	-4.2%
B6-2	June2020	6.16	+Bor	+0.6%
B7-1	June2020	8.16	+Bor	-4.8%
B8-1	June2020	7.93	+Bor+NaCl	-9.9%
B9-1	June2020	7.83	+Bor+NaCl+NaBr	-6.0%
C1-1	Jan2021	7.55	None	-7.0%
C1-2	Jan2021	7.54	None	-8.7%
C2-1	Jan2021	7.99	+Bor+NaCl+NaBr	-7.2%
C2-2	Jan2021	8.00	+Bor+NaCl+NaBr	-8.4%
C3-1	Jan2021	8.06	+Carb+NaCl	-6.6%
C3-2	Jan2021	8.06	+Carb+NaCl	-4.8%
C4-1	Jan2021	8.09	+Carb+NaCl+NaBr	-6.6%
C4-2	Jan2021	8.13	+Carb+NaCl+NaBr	-8.9%
C5-1	Jan2021	7.34	+NaCl+NaI	-2.4%
C5-2	Jan2021	7.34	+NaCl+NaI	-2.2%
C6-1	Jan2021	8.15	+Carb+NaCl+NaI	-9.4%
C6-2	Jan2021	8.16	+Carb+NaCl+NaI	-10.4%
C7-1	Jan2021	8.12	+Carb+NaCl+NaBr+NaI	-9.9%
C7-2	Jan2021	8.11	+Carb+NaCl+NaBr+NaI	-7.9%
C7-3	Jan2021	8.03	+Carb+NaCl+NaBr+NaI	-9.4%
C7-4	Jan2021	8.04	+Carb+NaCl+NaBr+NaI	-9.3%

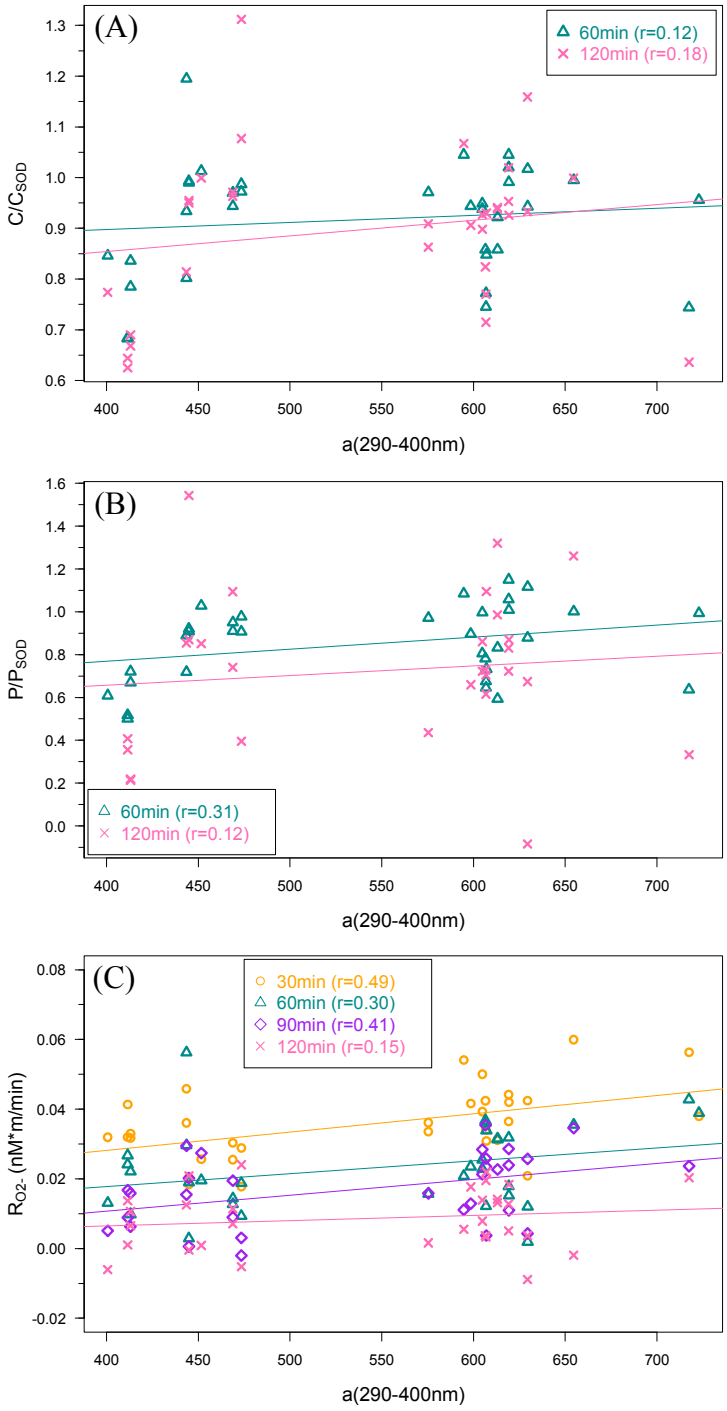

Figure S5. Superoxide decay ratios and photoproduction rates relative to CDOM $a_{(290–400)}$. A) C/C_{SOD} is not significantly correlated to $a_{(290–400)}$ (60: r=0.12, p=0.499; 120: r=0.18, p=0.316). B) P/P_{SOD} is not significantly correlated to $a_{(290–400)}$ (60: r=0.31, p=0.080; 120: r=0.115, p=0.558). C) R_{O2-} is not significantly correlated to $a_{(290–400)}$, except 60–90min (r=0.41, p=0.020).

Table S2. T-tests across chemical variables.

(A) Concentration Ratio, C/C_{SOD}

t-test	Time (min)	Mean Difference	t	df	p-value
None vs. Salt	60	+0.225	6.9	4.9	0.001*
	120	+0.428	5.0	2.7	0.021*
borate vs. carbonate	60	-0.025	1.7	4.6	0.149
	120	-0.015	0.5	2.1	0.675
SW-like vs. Br	60	-0.070	2.0	1.3	0.243
	120	-0.002	0.1	2.0	0.957
SW-like vs. I	60	+0.073	4.1	3.0	0.026*
	120	+0.045	1.0	2.5	0.404
SW-like vs. Br+I	60	+0.014	0.6	5.3	0.545
	120	+0.040	0.6	4.3	0.582

(B) Rate Ratio, P/P_{SOD}

t-test	Time Interval (min)	Mean Difference	t	df	p-value
None vs. Salt	0–60	+0.348	6.5	2.3	0.016*
	60–120	-0.155‡	—	—	—
borate vs. carbonate	0–60	+0.023	0.5	3.4	0.672
	60–120	-0.103	0.3	3.4	0.749
SW-like vs. Br	0–60	-0.237	1.8	1.3	0.265
	60–120	+0.205	0.9	2.6	0.452
SW-like vs. I	0–60	+0.155	2.3	3.1	0.099
	60–120	-0.171	1.9	2.0	0.193
SW-like vs. Br+I	0–60	+0.026	0.4	5.9	0.736
	60–120	-0.419	1.6	5.0	0.175

(C) Max Superoxide Rate, R_{O2^-}					
t-test	**Time Interval (min)**	**Mean Difference**	**t**	**df**	**p-value**
None vs. Salt	0–30	-0.00592	0.5	3.1	0.658
	30–60	-0.00974	1.1	4.1	0.320
	60–90	-0.01547	2.5	5.0	0.054
	90–120	-0.00119	0.1	4.0	0.916
borate vs. carbonate	0–30	+0.02379	3.7	4.9	0.014*
	30–60	+0.01912	3.2	4.3	0.031*
	60–90	+0.01469	2.0	3.3	0.136
	90–120	-0.00256	0.3	3.7	0.759
SW-like vs. Br	0–30	-0.01557	3.0	3.0	0.057
	30–60	0.00073	0.2	3.0	0.862
	60–90	-0.00541‡	—	—	—
	90–120	0.00704	1.5	2.1	0.266
SW-like vs. I	0–30	-0.00650	1.0	3.8	0.374
	30–60	-0.00582	0.7	1.6	0.556
	60–90	-0.00185	0.4	3.0	0.710
	90–120	+0.00230	0.4	2.9	0.728
SW-like vs. Br+I	0–30	-0.01006	1.4	6.0	0.222
	30–60	-0.01751	3.0	5.9	0.026*
	60–90	-0.01461	2.5	5.0	0.056
	90–120	+0.00110	0.1	4.9	0.896

‡ Not enough data was available to perform a t-test